Title Page

Neutral Sphingomyelinase Inhibition Alleviates LPS Induced Microglia Activation and Neuroinflammation after Experimental Traumatic Brain Injury

Asit Kumar[1], Rebecca J Henry, Bogdan A Stoica, David J Loane, Gelareh Abulwerdi, Shahnawaz A Bhat, Alan I Faden

Department of Anesthesiology and Shock, Trauma and Anesthesiology Research (STAR) Center, University of Maryland School of Medicine, Baltimore, MD, USA (A. K., R. J. H., B. A. S., D. J. L., G. A., S. A. B., A. I. F.)

[1]Current affiliation: Department of Neurology, Richard T Johnson Division of Neuroimmunology and Neurological Infections, Johns Hopkins University School of Medicine, Baltimore, MD, USA

Running Title Page

Running Title: Neutral Sphingomyelinase Inhibition Alleviates Neuroinflammation

Corresponding author: Dr. Alan I. Faden

Departments of Anesthesiology, Anatomy and Neurobiology, Neurosurgery, and Neurology, and Center for Shock, Trauma and Anesthesiology Research (STAR), University of Maryland School of Medicine, Baltimore, MD, USA

Tel: +1 410 706 4205

E-mail: afaden1@som.umaryland.edu

Co-corresponding author: Dr. Asit Kumar

E-mail: asitkumar14@gmail.com

Number of text pages including Abstract, main text, and footnote page: 25

Number of tables: 0

Number of figures: 9

Number of references: 107

Number of words in the Abstract: 209

Number of words in the Introduction: 685

Number of words in the Discussion: 2063

Abbreviations:

TBI, Traumatic brain injury

nSMase, Neutral sphingomyelinase

CCI, Controlled cortical injury

LPS, Lipopolysaccharide

MP, Microparticles

EV, Extracellular vesicles

TNF-α, Tumor necrosis factor-alpha

IL-1β, Interleukin-1β

IL-6, Interleukin 6, CCL2; C-C Motif Chemokine Ligand 2

IL-4ra, IL-4 receptor subunit alpha

Mrc1/CD206, Mannose receptor C-type 1/Cluster of Differentiation 206

Arg-1, Arginase 1

Ym1/Chil3, Ym1/Chitinase-like 3

NOS2/iNOS, Nitric Oxide Synthase 2/Inducible nitric oxide synthase

Nox2, NADPH oxidase 2

CD68, Cluster of Differentiation 68

MAPK, Mitogen-activated protein kinase

ERK, Extracellular signal–regulated kinase

JNK, c-Jun N-terminal kinase

IκBα, Nuclear factor of kappa light polypeptide gene enhancer in B-cells inhibitor, alpha

NF-κB, Nuclear factor kappa-light-chain-enhancer of activated B cells

miR, microRNA

Recommended section assignment: Neuropharmacology

Abstract

Neuroinflammation is one of the key secondary injury mechanisms triggered by traumatic brain injury (TBI). Microglial activation, a hallmark of brain neuroinflammation, plays a critical role in regulating immune responses after TBI and contributes to progressive neurodegeneration and neurological deficits following brain trauma. Here we evaluated the role of neutral sphingomyelinase (nSMase) in microglial activation by examining the effects of the nSMase inhibitors Altenusin and GW4869 *in vitro* (using BV2 microglia cells and primary microglia), as well as in a controlled cortical injury (CCI) model in adult male C57BL/6 mice. Pre-treatment of Altenusin or GW4869 prior to lipopolysaccharide (LPS) stimulation for 4 h or 24 h, significantly downregulated gene expression of the pro-inflammatory mediators TNF-α, IL-1β, IL-6, iNOS and CCL2 in microglia and reduced the release of Nitric Oxide and TNF-α. These nSMase inhibitors also attenuated the release of microparticles and phosphorylation of p38 MAPK and ERK1/2. In addition, Altenusin pre-treatment also reduced the gene expression of multiple inflammatory markers associated with microglial activation after experimental TBI - including TNF-α, IL-1β, IL-6, iNOS, CCL2, CD68, NOX2 and $p22^{phox}$. Overall, our data demonstrate that nSMase inhibitors attenuate multiple inflammatory pathways associated with microglial activation *in vitro* and after experimental TBI. Thus, nSMase inhibitors may represent promising therapeutics agents targeting neuroinflammation.

Keywords: Microglia, neuroinflammation, traumatic brain injury, neutral sphingomyelinase, extracellular vesicles.

Introduction

Recent clinical and experimental studies show that traumatic brain injury (TBI) initiates a sustained neuroinflammatory response with microglial activation that contributes to posttraumatic neurodegeneration and chronic neurological deficits (Loane and Byrnes, 2010; Loane *et al.*, 2014). Such neurotoxic microglial activation is associated with both phenotypic and genotypic changes (Loane and Kumar, 2016). The latter include activation of inflammatory cytokines, chemokines, and microRNAs (miRs) (Perry *et al.*, 2010; Prinz and Priller, 2014). Activated microglia also release extracellular vesicles (EVs), including microparticles (MP) and exosomes (Exo) containing pro-inflammatory molecules, which can further enhance and potentially propagate the inflammatory response after TBI (Hazelton *et al.*, 2018; Paolicelli *et al.*, 2018). Several *in vitro* and *in vivo* models, including lipopolysaccharide (LPS)-treated primary microglia, cell lines (e.g. BV2 microglia), and LPS challenged mice have been used to mimic such neurotoxic microglial activation (Loane *et al.*, 2009; Mao *et al.*, 2012; Fenn *et al.*, 2014; Yuan *et al.*, 2015; Hung *et al.*, 2017). The LPS model stimulates microglial activation pro-inflammatory phenotypic changes, and it has also been used in EVs studies whereby MP released from activated microglia are enriched in pro-inflammatory mediators such as interleukin-1β (IL-1β) (Kumar *et al.*, 2017; Yang *et al.*, 2018). Experimental neuroprotection strategies for TBI have included modulation of upstream activation mechanisms using NADPH-oxidase (NOX2) inhibitors or mGluR5 agonists (Loane *et al.*, 2013; Kumar *et al.*, 2016; Kumar *et al.*, 2016), as well as strategies serving to inhibit the release of specific inflammatory factors such as pro-inflammatory cytokines (Kumar *et al.*, 2016). We have recently shown in a murine experimental TBI model that neutralization of EVs using a novel surfactant polyethylene glycol telomere B (PEG-TB) can serve to reduce the release of pro-

inflammatory factors (Kumar *et al.*, 2017); this treatment was also found to be neuroprotective in a porcine model of TBI (Bohman *et al.*, 2016).

A number of studies have also begun to examine the effects of nSMase inhibitors, such as Altenusin and GW4869, on brain immune cell function and as potential anti-inflammatory agents (Iguchi *et al.*, 2016; Chua *et al.*, 2017; Dickens *et al.*, 2017; Huang *et al.*, 2018; Sobue *et al.*, 2018). The nSMases are a family of sphingomyelin phosphodiesterase enzymes that catalyze hydrolysis of sphingomyelin (SM), a major component of eukaryotic cell membrane, to produce phosphocholine and ceramide (Wu *et al.*, 2010; Figuera-Losada *et al.*, 2015). Regulation of innate immune responses mediated through nSMase inhibition might provide beneficial effects for several neurodegenerative diseases (Guo *et al.*, 2015; Dinkins *et al.*, 2016; Bilousova *et al.*, 2018). Prior studies demonstrate that nSMase inhibitors can limit neuroinflammation and neuronal cell-death (Brann *et al.*, 2002). Thus, such drugs can protect neurons, astrocytes, and oligodendrocytes against ceramide induced-cell death produced by pro-inflammatory molecules (tumor necrosis factor-α; TNF-α), β-Amyloid, and cerebral ischemia (Luberto *et al.*, 2002; Lee *et al.*, 2004; Zeng *et al.*, 2005; Martinez *et al.*, 2012; Gu *et al.*, 2013). Recent studies indicate that myeloid cells can release EVs/MP that spread inflammatory signals both *in vitro* and *in vivo* to alter neuronal functions (Harrison-Brown *et al.*, 2016; Nigro *et al.*, 2016; Beneventano *et al.*, 2017; Kumar *et al.*, 2017). Importantly, EVs levels are significantly increased following TBI in humans and animal models, as well as in chronic neurodegenerative and autoimmune disorders such as Alzheimer's disease (AD) and multiple sclerosis, supporting the concept that spreading inflammation via EVs release may play a role in these neuropathologies (Taylor and Gercel-Taylor, 2014; Xiao *et al.*, 2017; Pieragostino *et al.*, 2018). Thus, nSMase inhibitors have emerged as new pharmacological agents for preventing release of EVs and thus can modulate inflammation and oxidative stress.

In the present study, we investigated the therapeutic potential of the nSMase inhibitors Altenusin and GW4869 in BV2 murine microglial cell line and primary microglia *in vitro*, as well as in the mice subjected to controlled cortical impact (CCI), a well-characterized experimental TBI model. More specifically, we examined their ability to modulate LPS induced microglial activation, as well as release of pro-inflammatory molecules and EVs *in vitro*, and on markers of secondary neuroinflammation following TBI in mice. In addition, we evaluated the potential underlying signal transduction mechanisms involved.

Materials and Methods

Animals: Studies were performed using 10-12 weeks old C57BL/6 male mice (Taconic Biosciences, Germantown, NY; 22–26 g wt.). Mice were housed in the Animal Care Facility at the University of Maryland School of Medicine under standard laboratory conditions, maintained on 12 h light/dark cycle with temperature of 24°C, with *ad libitum* access to food and water. Mice were acclimatized in the animal surgery room half an hour before the surgery. All surgical procedures were performed in accordance with protocols approved by the Institutional Animal Care and Use Committee (IACUC) at the University of Maryland School of Medicine.

Controlled cortical impact: Brain injury in mice was induced using our custom-designed CCI injury device consists of a microprocessor-controlled pneumatic impactor with a 3.5 mm diameter tip as described previously (Kabadi *et al.*, 2012). Briefly, mice were anesthetized in gas chamber containing evaporated mixture of gases 70% N_2O and 30% O_2 along with isoflurane (induction at 4% and maintenance at 2%) and directed through a nose mask. Depth of anesthesia was assessed, before initiation of the surgical procedure, by monitoring respiration rate and pedal withdrawal reflexes. Animals were placed on a heated pad to maintain a body temperature of 37°C under the

anesthesia. The head was mounted in a stereotaxic frame and a 10 mm midline incision was made over the skull. After reflecting the skin and fascia, a 5 mm craniotomy was made on the central aspect of the left parietal bone. The impounder tip of the injury device was positioned to the surface of the exposed dura after extending to its full stroke distance (44 mm) and reset to impact the cortical surface. Moderate injury was induced using an impactor velocity of 6 m/sec and deformation depth of 2 mm. After performing the CCI injury, the incision was closed with interrupted 6-0 silk sutures. Following anesthesia withdrawal, the animal was placed into a heated cage for at least 45 min post-injury to maintain the normal body temperature. All animals were monitored carefully for at least 4 hours after surgery. Sham animals underwent the same procedure as injured mice except for craniotomy and cortical impact.

***In vivo* drug Treatments**: At 30 min post-injury injured mice received a single intraperitoneal (i.p.) injection of altenusin (Millipore Sigma) at 2 mg/kg or 10 mg/kg in saline + dimethyl sulphoxide (DMSO; Millipore Sigma), or equal volume of vehicle (saline + DMSO). Drug dosage were partly based upon prior *in vivo* studies for altenusin in mice (Chua *et al.*, 2017). At 24 h post-injury mice were humanely euthanized, and brain tissues were rapidly dissected and stored at -80°C following transcardial perfusion with ice-cold sterile phosphate buffered saline (PBS).

BV-2 cell culture: BV2 murine microglial cells were cultured in Dulbecco's modified Eagle's medium (DMEM; Life Technologies) supplemented with 10% fetal calf serum (Life Technologies) and 1% penicillin and streptomycin (40 U/mL and 40 µg/mL, respectively; Millipore Sigma) at 37°C with 5% CO_2. Cells were split 1:5 until their confluency using 0.05% Trypsin-EDTA (Life Technologies) solution in phosphate buffered saline (PBS). For activation of BV-2 microglia, lipopolysaccharide (LPS from Escherichia coli; 20 ng/mL; Millipore Sigma) was used. BV2 microglia were seeded at a density of either 3×10^5 cells/well (6-well plate), 1.5×10^5

cells/well (12-well plate), 0.75×10^5 cells/well (24-well plate) or 20,000 cells/well (96-well plate). Cell were incubated with or without various concentration of Altenusin (10 - 100 μM) or GW4869 (1 – 10 μM; Millipore Sigma) followed by LPS stimulation (20 ng/ml) for either 4 h or 24 h.

Primary microglia cultures: Primary microglia cultures were prepared from cerebral cortices of postnatal day P1-3 Sprague-Dawley rats as previously described (Olajide *et al.*, 2014; Singh *et al.*, 2014). In brief, brains were carefully taken, and cerebral cortices were collected and freed from meninges in Hanks' Balanced Salt Solution (HBSS; without Calcium, Magnesium and Phenol Red; Life Technologies). Forebrains were minced and gently dissociated by repeated pipetting in DMEM/F-12 medium (Life Technologies) and filtered by passing through 70 μm cell strainer (Millipore Sigma). Cells were collected by centrifugation (1000 x g, 10 min at 4°C) and resuspended in DMEM/F-12 containing 10% fetal calf serum (Life Technologies) and 1% penicillin and streptomycin (40 U/mL and 40 μg/ml, respectively) and cultured on Poly-D-lysine coated 75 cm^2 cell culture flask (Millipore Sigma) in 5% CO_2 at 37°C. After 12–14 days in culture, floating microglia were harvested from mixed glia (astrocyte-microglia) cultures and re-seeded into cell culture plates at the density of either 0.75×10^5 cells/well (24-well plate) or 1.5×10^5 cells/well (12-well plate). On the next day, non-adherent cells were removed by changing the media, and after 1 h cells were used for experiments. Cells were incubated with altenusin (10 - 50 μM) followed by LPS stimulation (20 ng/ml) for either 4 h or 24 h.

Cell viability assay: Cell viability was determined using a tetrazolium salt 3-(4,5-dimethylthiazol-2-yl)-2,5-diphenyltetrazolium bromide (MTT; Millipore Sigma) colorimetric assay (Mosmann, 1983). BV2 microglia cells were incubated in 96 well plates in DMEM containing 10% fetal calf serum and 1% penicillin and streptomycin (40 U/mL and 40 μg/mL, respectively) containing various concentrations of altenusin and GW4869 for 24 h. 10 μl of MTT at a final concentration

JPET Fast Forward. Published on December 18, 2018 as DOI: 10.1124/jpet.118.253955
This article has not been copyedited and formatted. The final version may differ from this version.

of 0.5 mg/ml were added to each well. After 3 h incubation in 5% CO_2 at 37°C, media was discarded, and formazan crystals were dissolved by adding 100 µl of DMSO to each well. The absorbance was measured at 540 nm using absorbance microplate reader (Biotek) and is directly proportional to cell viability. Cell viability was expressed as a percentage of surviving cells compared with the non-stimulated control cells.

mRNA real-time PCR: RNA was isolated using Direct-zol™ RNA mini prep kit (ZYMO Research). For cDNA synthesis, total RNA was reverse transcribed using High-Capacity cDNA Reverse Transcription Kit (ThermoFisher Scientific) as per manufacturer's instructions. In brief, each 20 µl of RT reaction consisted of 2 µl of 10X RT Buffer, 0.8 µL of 25X dNTP Mix (100 mM), 2.0 µL of 10X RT Random Primers, 1.0 µL of MultiScribe™ Reverse Transcriptase, 4.2 µL of Nuclease-free water and 10µl of RNA sample. Thermal cycling conditions used for reverse transcription are 10 min at 25°C, 120 min at 37°C and finally 5 min at 85°C followed by stop at 4°C. The synthesized cDNA was the template for the real-time PCR amplification that was carried out either by ABI 7900HT or Quant Studio™ 5 real-time PCR System (ThermoFisher Scientific), using TaqMan Universal Master Mix II, no UNG (ThermoFisher Scientific) as per the company's protocol. Reaction conditions were 10 min at 95°C, followed by 40 cycles of 15 s at 95°C, 60 s at 60°C, followed by the final plate read. The following primers were used in this study: Mm00443258_m1 TNF-α (mouse), Rn01525859_g1 TNF-α (rat), Mm00446190_m1 IL-6 (mouse), Rn01410330_m1 IL-6 (rat), Mm01336189_m1 IL-1β (mouse), Rn00580432_m1 IL-1β (rat), Mm00440502_m1 Nos2/iNOS (mouse), Rn00561646_m1 Nos2/iNOS (rat), Mm00441242_m1 CCL2 (mouse), Rn00580555_m1 CCL2 (rat), Mm01288386_m1 IL-10 (mouse), Mm99999915_g1, GAPDH (mouse), Rn01775763_g1 GAPDH (rat), Mm03047343_m1 CD68 (mouse), Mm01287743_m1 CYBB/NOX2 (mouse), Mm00514478_m1 CYBA/$p22^{phox}$

JPET Fast Forward. Published on December 18, 2018 as DOI: 10.1124/jpet.118.253955
This article has not been copyedited and formatted. The final version may differ from this version.

(mouse), Mm01275139_m1 IL4ra (mouse), Mm01329362_m1 Mrc1/CD206 (mouse), Mm00475988_m1 Arg-1 (mouse), Mm00657889_mH Ym1/Chil3 (mouse). GAPDH served as an internal control for sample normalization and the comparative cycle threshold method ($2^{-\Delta\Delta Ct}$) was used for data quantification as described previously (Livak and Schmittgen, 2001).

microRNA real-time PCR: Following RNA isolation using Direct-zol™ RNA mini prep kit (ZYMO Research), miRNAs were reverse-transcribed by using TaqMan® microRNA reverse transcription kit (ThermoFisher Scientific) according to manufacturer's protocol. In brief, the master mix of 7 µl contained 1.5 µl of Reverse Transcription Buffer (10X), 0.15 µl of dNTPs (100 mM; with Deoxythymidine triphosphate), 1 µl of MultiScribe™ Reverse Transcriptase (50 U/µl), 0.19 µl of RNase Inhibitor (20 U/µl), and 4.16 µl Nuclease-free water. Each 15 µl of RT reaction consisted of 7 µl of master mix, 3 µl of RT primer (5X), and 5 µl of RNA sample (10 ng). Thermal cycling conditions used for reverse transcription are 30 min at 16°C, 30 min at 42°C and finally 5 min at 85°C followed by stop at 4°C. For real-time PCR amplification of mature miRNA, TaqMan® Universal PCR master mix II (2X) with no UNG, and TaqMan® Small RNA assays (20X) were used according to manufacturer's protocol. mmu480953_mir miR-155, mmu478399_mir miR-146a, 001973 U6 snRNA. In brief, the reaction setup for real-time PCR of 20 µl contained 10 µl of TaqMan Universal PCR master mix II (2X), 1 µL of TaqMan Small RNA assay (20X), 1.33 µl of Template cDNA, and 7.67 of µl Nuclease-free water. The cycling condition for real-time PCR involved 40 cycles started with PCR initial enzyme activation step for 10 min at 95°C and then 15 s at 95°C and 60 s at 60°C. The real-time qPCR results were normalized to RNU6 (Life technologies) and quantified using comparative Ct method $2^{-\Delta\Delta Ct}$ (Livak and Schmittgen, 2001). PCR reactions were carried out either by ABI 7900HT or Quant Studio™ 5 real-time PCR System (ThermoFisher Scientific).

Microparticle analysis by flow cytometry: Microparticles (MP), a special class of extracellular vesicles released into BV2 microglial media were characterized using a MACSQuant flow cytometer (Miltenyi Biotec) as described previously (Kumar *et al.*, 2017). For MP analysis, fetal calf serum (Life Technologies) was subjected to 18 h centrifugation at 100,000×g. DMEM media was filtered using 0.22-μm filter (Millipore). Cells were pre-treated with altenusin and GW4869 for 30 min followed by LPS stimulation for 24 h. To induce the MP shedding, cells were conditioned with 100 μM of BzATP for 30 min. At the end of the experiment, cell supernatants were used to collect total MP that were purified by using ultra centrifugation at the speed of 300xg for 10 min, 2100xg for 10 min followed by 100,000xg for 1 h at 4°C as previously described (Shet *et al.*, 2004; Erdbruegger, 2010; Poncelet *et al.*, 2015; Tian *et al.*, 2015; Kumar *et al.*, 2017) with minor modification. To characterize the size of MP, MACSQuant was first calibrated with calibration beads (Miltenyi Biotec), and forward and side scatters were set at logarithmic gain. Photomultiplier tube voltage and triggers were optimized to detect submicron-sized particles. Microbead standards of various sizes 300 nm (Sigma; LB3), 1090 nm (Spherotech; BCP-10-5), and 3000 nm (Spherotech; BP-30-5) were used to set the initial parameters in the flow cytometer. MP were distinguished from larger (apoptotic body; >1000 nm) and smaller (exosomes; <100 nm) vesicles based on size (SSC), and their phenotype was confirmed using the APC-conjugated Annexin V (Catalog No. 550474; BD Bioscience). All reagents and solutions used for MP analysis were sterile and filtered (0.1 μm or 0.22 μm filter; Millipore) before use.

Western blotting: To generate whole-cell extracts, cells were washed with cold PBS and lysed in the radioimmunoprecipitation assay buffer (RIPA buffer; Teknova), with 3% phosphatase (Phosphatase Inhibitor Cocktail 2 & 3; Millipore Sigma) and protease inhibitor cocktail (Millipore Sigma). Protein concentration of the samples was measured using the bicinchoninic acid (BCA)

JPET Fast Forward. Published on December 18, 2018 as DOI: 10.1124/jpet.118.253955
This article has not been copyedited and formatted. The final version may differ from this version.

protein assay kit (ThermoFisher Scientific) according to the manufacturer's instructions. For Western blotting, 15 μg of total protein from each sample was subjected to 5–20% gradient gels for sodium dodecyl sulfate-polyacrylamide gel electrophoresis (SDS-PAGE). Proteins were transferred onto nitrocellulose membranes and blocked in 5% BSA in tris-buffered saline (TBS) containing 0.1% Tween 20 (TBS-T). After blocking, membranes were incubated with primary antibodies, including phospho-p38 MAPK (1:1000; Cell Signaling Technology), phospho-ERK1/2 (1:1000; Cell Signaling Technology), phospho-JNK (1:1000; Cell Signaling Technology), anti-IκB-α (1:1000; Cell Signaling Technology), and rabbit anti-actin (1:5000; Cell Signaling Technology). Primary antibodies were diluted in TBS-T and 5% BSA. Membranes were incubated with the primary antibody overnight at 4°C followed by incubation in appropriate HRP-conjugated secondary antibodies (Jackson Immuno Research Laboratories) for 1 h at room temperature. After extensive washing (three times for 15 min each in TBS-T), proteins were visualized using Super Signal West Dura Extended Duration Substrate (ThermoFisher Scientific). Chemiluminescence was captured using ChemiDoc TM XRS+ System (Bio-Rad). Densitometry analyses of the proteins were performed using ImageJ software (NIH, USA), and β-actin was used to confirm equal sample loading and normalization of the data.

Nitrite release: Nitrite levels in cell culture supernatant was measured using a Griess reagent kit (ThermoFisher Scientific) according to manufacturer's instruction. Absorbance was measured at 548 nm using the Synergy™ HT multi-mode microplate reader (Biotek) and normalized with the reference sample. Amount of Nitrite (expressed in μM) released by microglia cells in each sample was calculated by plotting standard curve.

Determination of TNF-α release from LPS-activated microglia: Levels of TNF-α released in BV2 and primary rat microglia cell culture supernatant were measured using mouse and rat ELISA

kit from R&D Systems and BD biosciences, respectively, as per manufacturer's instructions. Briefly, standards or samples were added to antibody-coated 96-well plates and incubated for 2 h at RT. After washing the plates with wash buffer, samples were incubated with detection antibody for another 2 h at RT. Plates were washed and incubated in HRP-conjugated streptavidin for 20 min at RT in dark. Substrate solution was added, and plate was left for incubation 30 min in the dark. After the incubation, stop solution was added and absorbance was measured at 450 nm using a Synergy™ HT Multi-Mode Microplate Reader (Biotek). A standard curve was used to calculate the levels of TNF-α release and expressed as picograms of cytokine/milliliters.

Statistical analysis: Statistical analyses were performed using GraphPad Prism software (GraphPad Software Inc., San Diego, CA, USA). Values of all experiments are represented as mean ± SEM of at least three independent experiments. Values were compared using one-way analysis of variance (ANOVA) with Tukey's post hoc correction (multiple comparisons). The level of significance was set at $*P < 0.05$, $**P < 0.01$, $***P < 0.001$.

Results

Effects of Altenusin and GW4869 on the microglial cell viability

To determine the cytotoxic potential of altenusin (**Fig. 1A**) and GW4869 (**Fig. 1B**), the viability of BV2 microglia was evaluated using an MTT assay. Treatment with altenusin (ranging from 1-100 μM) prior to LPS stimulation (20 ng/ml) did not adversely affect BV2 microglia viability, when compared to control or unstimulated cells (**Fig. 1C**). Similarly, pre-treatment of GW4869 (ranging from 1- 10 μM) did not affect microglial cell viability (**Fig. 1D**), however, 20 μM GW4869 with ($P < 0.05$) and without LPS ($P < 0.01$) significantly decreased cell viability, indicating GW4869 cytotoxicity > 10 μM.

JPET Fast Forward. Published on December 18, 2018 as DOI: 10.1124/jpet.118.253955
This article has not been copyedited and formatted. The final version may differ from this version.

Altenusin and GW4869 attenuate LPS-induced activation of BV2 microglia

To investigate whether altenusin and GW4869 exerts anti-inflammatory effects, BV2 microglia were pre-incubated with altenusin and GW4869 for 30 min and then stimulated with or without LPS. We evaluated gene expression levels of key pro-inflammatory cytokines (TNF-α, IL-1β, and IL-6), inducible form of nitric oxide synthase (iNOS), chemokine (CCL2) and the anti-inflammatory cytokine (IL-10). Based on time-course analysis (data not shown), we identified the time point for mRNA analysis to be 4 h post-LPS stimulation when pro-inflammatory mRNAs were robustly induced. LPS stimulation of BV2 microglia significantly increased the expression of TNF-α (LPS *vs* control, $P < 0.001$), IL-1β (LPS *vs* control, $P < 0.001$), IL-6 (LPS *vs* control, $P < 0.001$), iNOS (LPS *vs* control, $P < 0.001$), and CCL2 (LPS *vs* control, $P < 0.001$) (**Fig. 2A-E**). Pre-treatment of altenusin significantly reduced expression of TNF-α (**Fig. 2A**) and IL-6 (**Fig. 2B**) at 75 μM (TNFα, $P < 0.001$; IL-6 $P < 0.001$) and 100 μM (TNF-α, $P < 0.001$; IL-6 $P < 0.001$), as compared to LPS alone. Altenusin also significantly decreased expression of IL-1β (**Fig. 2C**), iNOS (**Fig. 2D**) and CCL2 (**Fig. 2E**), starting at 50 μM (LPS *vs* LPS + altenusin; IL-1β, $P < 0.001$; iNOS $P < 0.001$; CCL2 $P < 0.01$). Similarly, pre-treatment of GW4869 for 30 min significantly reduced gene expression of TNF-α (5 μM – 10 μM, $P < 0.001$; **Fig. 2G**), IL-6 (5 μM – 10 μM, $P < 0.001$; **Fig. 2H**), IL-1β (5 μM – 10 μM, $P < 0.001$; **Fig. 2I**), iNOS (10 μM, $P < 0.05$, **Fig. 2J**), CCL2 (5 μM – 10 μM, $P < 0.001$; **Fig. 2K**) following LPS stimulation. Altenusin and GW4869 did not significantly increase IL-10 gene expression following LPS stimulation (**Fig. 2F, 2L**).

With regard to protein markers, peak expression of TNF-α and nitric oxide production in BV2 and primary microglia is at 24 h following LPS stimulation (Loane *et al.*, 2014; Stoica *et al.*, 2014; Kumar *et al.*, 2017). As predicted, we observed a significant increase in the nitrite levels

and TNF-α protein in the supernatant of BV2 stimulated with LPS at 24h as compared to control treated cells (**Fig. 3A-D**). Altenusin pretreatment significantly decreased nitrite production in a dose dependent manner, starting at 25 µM (LPS *vs* LPS + altenusin; $P < 0.001$; **Fig. 3A**). Similarly, GW4869 pretreatment significantly reduced nitrite release following LPS stimulation, starting at 5 µM (LPS *vs* LPS + GW4869; $P < 0.001$; **Fig. 3B**). Altenusin and GW4869 treatment did not significantly change the nitrite levels when added to BV2 microglia in the absence of LPS. Pretreatment of altenusin significantly decreased TNF-α protein levels following LPS stimulation, starting at 75 µM (LPS *vs* LPS + altenusin; $P < 0.001$; **Fig. 3C**), whereas TNF-α levels were significantly decreased following GW4869 treatment at 10 µM (LPS *vs* LPS + GW4869; $P < 0.05$; **Fig. 3D**).

Altenusin attenuate LPS-induced activation of primary microglia

To confirm the data obtained from BV2 microglial cells, we also tested the anti-inflammatory properties of altenusin in primary rat microglia. In response to LPS stimulation we observed a robust increase in the mRNA levels of TNF-α (LPS *vs* control, $P < 0.001$), IL-6 (LPS *vs* control, $P < 0.001$), IL-1β (LPS *vs* control, $P < 0.01$), iNOS (LPS *vs* control, $P < 0.001$), and CCL2 (LPS *vs* control, $P < 0.01$; **Fig. 4A-E**). Pre-treatment with altenusin resulted in a significant downregulation of TNF-α (**Fig. 4A**), IL-6 (**Fig. 4B**) and iNOS (**Fig. 4D**) starting at 10 µM (TNFα, $P < 0.001$; IL-6 $P < 0.001$; iNOS $P < 0.001$), whereas IL-1β (**Fig. 4C**) and CCL2 (**Fig. 4E**) expression were significantly decreased starting at 25 µM (IL-1β, $P < 0.05$; CCL2, $P < 0.01$) and 50 µM (IL-1β, $P < 0.01$; CCL2, $P < 0.01$) of altenusin. Next, we investigated the LPS-induced release of nitrite and TNF-α in primary rat microglia (**Fig. 5A, B**). LPS stimulation resulted in a significant increase in the release of nitrite (**Fig. 5A**) and TNF-α protein (**Fig. 5B**). Pretreatment

with altenusin significantly reduced nitrite levels starting at 10 μM (LPS *vs* LPS + altenusin; $P < 0.001$; **Fig. 5A**), whereas levels of TNF-α protein was significantly reduced starting at 25 μM (LPS *vs* LPS + altenusin; $P < 0.001$; **Fig. 5B**).

Altenusin and GW4869 attenuate LPS-induced elevation of pro-inflammatory miR-155

We assessed changes in pro-inflammatory miR-155 and miR-146 levels in BV2 microglia pretreated with altenusin and GW4869 and stimulated with LPS (**Fig. 5C, 5D**). Altenusin or GW4869 treatment prior to LPS stimulation significantly decreased miR-155 expression at 100 μM altenusin ($P < 0.01$ *vs* LPS) and at 10 μM GW4869 ($P < 0.01$ *vs* LPS) (**Fig. 5C**), respectively, but these inhibitors had no significant effects on LPS-induced miR-146 expression (**Fig. 5D**).

Effects of Altenusin and GW4869 on the microparticle release induced by combined treatment with LPS and BzATP

Next, we investigated if altenusin and GW4869 had any effect on the MP release in activated microglia (**Fig. 6**). P2X7 triggers MP shedding in the microglia, which can be activated by agonists such as ATP or BzATP (synthetic analogue of ATP) (Bianco *et al.*, 2005, 2009). Therefore, BV2 microglia were pretreated with altenusin and GW4869 for 30 min and then stimulated with or without LPS for 24 h followed by an additional BzATP stimulation for 30 min to induce MP shedding (Kumar *et al.*, 2017). MP were quantified by flow cytometry using annexin V, which binds the externalized phosphatidylserine (PS) present on the MP surface. Apoptotic bodies (> 1000 nm) and exosomes (< 100 nm) were excluded by gating analysis, and MP ranging in size between 300-1000 nm were analyzed (**Fig. 6A**). LPS/BzATP significantly induced the shedding of annexin V positive MP compared to MP levels in control BV2 microglia ($P < 0.001$;

Fig 6B). Interestingly, we found that altenusin (50 µM and 100 µM) and GW4869 (5 µM and 10 µM) significantly decreased the microparticle count ($P < 0.001$) in the activated BV2 microglia.

Altenusin inhibits the pro-inflammatory pathways p38 MAPK and ERK1/2

Mitogen-activated protein kinase (MAPK) pathways are implicated in several cellular processes including neuroinflammation (Kaminska, 2005; Kaminska *et al.*, 2009). To further investigate the mechanism by which altenusin modulates cytokines production, we assessed altenusin effects on the activation of various components of MAPK in LPS-activated BV2 microglia (**Fig. 7A**). LPS treatment of microglia for 30 min led to the phosphorylation, and thus activation of p38 MAPK ($P < 0.001$), ERK1/2 ($P < 0.05$), and JNK ($P < 0.001$) (**Fig. 7B-D**). Notably, pretreatment of altenusin at 100 µM significantly reduce phosphorylation of p38 ($P < 0.05$ *vs* LPS; **Fig. 7B**). Similarly, there was a significant reduction in the phosphorylation of ERK1/2 by altenusin ($P < 0.05$ *vs* LPS; **Fig. 7C**). In contrast, altenusin failed to reduce LPS-stimulated phosphorylation of JNK (**Fig. 7D**), or degradation of IκBα (**Fig. 7E**).

Systemic treatment of altenusin attenuates acute neuroinflammation following experimental traumatic brain injury in mice

We then investigated whether altenusin has similar anti-inflammatory properties *in vivo*. We used a well-established model of CCI in adult male C57BL/6 mice to induce a cortical focal contusion injury and examined whether the increases in gene expression of proinflammatory cytokines and chemokines were ameliorated by altenusin treatment. 2 mg/kg and 10 mg/kg of altenusin was administered systemically (i.p.) to moderate-level CCI mice starting at 30 minutes post-injury (**Fig. 8A**). Sham and CCI mice were euthanized 24 hours later, and cortical tissue was

collected for mRNA analysis of TNFα, IL-6, IL-1β, iNOS, CCL2, CD68, NOX2 and $p22^{phox}$. Following CCI there was a robust increase in mRNA for pro-inflammatory mediators TNFα, IL-6, IL-1β, iNOS, and CCL2 ($P < 0.001$ *vs* sham; **Fig. 8B-F**). Altenusin (10 mg/kg) treatment significantly reduced the expression levels of TNF-α ($P < 0.01$; **Fig. 8B**), IL-6 ($P < 0.05$; **Fig. 8C**), IL-1β ($P < 0.05$; **Fig. 8D**), iNOS ($P < 0.05$; **Fig. 8E**) and CCL2 ($P < 0.01$; **Fig. 8F**) when compared to vehicle-treated CCI group. We also evaluated the expression of CD68, a marker of activated and phagocytic microglia (Song *et al.*, 2011; Fu *et al.*, 2014; Walker and Lue, 2015). CD68 expression was significantly increased in the vehicle-treated CCI group ($P < 0.05$ vs sham; **Fig. 8G**), and its expression was significantly reduced with altenusin (10 mg/kg) treatment ($P < 0.05$ vs Vehicle-treated CCI). NOX2 has been implicated in microglial-mediated neurotoxicity in TBI (Loane *et al.*, 2014; Kumar *et al.*, 2016), so we analyzed the gene expression of NOX2 and $p22^{phox}$ in the injured cortex. There was a significant increase in the expression of NOX2 and $p22^{phox}$ mRNA expression with CCI ($P < 0.001$ *vs* sham; **Fig. 8H, 8I**), and altenusin treatment (10 mg/kg) significantly reduced both subunit expression ($P < 0.05$ *vs* Vehicle-treated CCI).

Finally, to investigate whether Altenusin has modulatory effects on anti-inflammatory and pro-resolution immune responses we assessed anti-inflammatory and alternative activation microglial markers (IL-10, IL-4ra, Arg-1, Mrc1/CD206, and Ym1/Chil3). CCI induced significant increase in IL-10, IL-4ra, Arg-1 mRNA expression in the injured cortex ($P < 0.05$-0.001 *vs* sham; **Fig. 9A, 9B, 9D**), as well as increased Mrc1/CD206 and Ym1/Chil3 expression that failed to reach statistical significance (**Fig. 9C, 9E)**. Post-injury treatment of altenusin at both doses (2 and 10 mg/kg) did not increase expression of these anti-inflammatory and pro-resolving genes in the injured cortex beyond vehicle-treated CCI levels (**Fig. 9A-E**).

Discussion

In the present study we demonstrate the anti-inflammatory effects of nSMase inhibitors in activated microglia *in vitro* and in an experimental TBI model in mice. Altenusin and GW4869 significantly suppressed neuroinflammation - reducing the gene expression of proinflammatory cytokines (TNFα, IL-1β, IL-6), chemokines (CCL2) and iNOS, as well as microglia activation markers (CD68) and components of NADPH Oxidase (NOX2, $p22^{phox}$). They also reduced the extracellular release of TNF-α and nitric oxide in activated BV2 cells and primary microglia. These inflammatory molecules are known to be important mediators of microglial activation and neuroinflammation associated with several neurological conditions, including TBI (Hanisch, 2002; Woodcock and Morganti-Kossmann, 2013; Thelin *et al.*, 2017).

GW4869 is a selective, non-competitive nSMase2 inhibitor that shows no inhibitory activity on acid sphingomyelinase (aSMase) (Luberto *et al.*, 2002), whereas altenusin is a non-steroidal fungal metabolite with broader nSMase inhibitor activity, known to target multiple isoforms of nSMase (Uchida *et al.*, 1999; Dickens *et al.*, 2017). In the current study we demonstrated that both nSMase inhibitors attenuated LPS-induced microglial activation and the release of pro-inflammatory mediators *in vitro*, although altenusin had greater potency and less cytotoxicity than GW4869. Some prior studies have demonstrated therapeutic effects of GW4869 at 20 μM in breast cancer cells, macrophages, and mesenchymal stem cells (Wu *et al.*, 2005; Essandoh *et al.*, 2015; Xiao *et al.*, 2018); however, in our studies 20 μM GW4869 significantly induced cytotoxicity, thereby negatively impacting microglial cell viability beginning at concentration of > 10 μM. The differences we identified in the GW4869 cytotoxicity profile compared to the above-mentioned studies may be due to the different cell types examined (microglia versus non-brain derived cells). Collectively, our data suggest that a more general

inhibition of nSMase activity may improve effectiveness. A limitation of pharmaceutical intervention approaches used to address potential mechanisms is that they may have off-target activity. For example, altenusin has been shown to have inhibitory effects on a number of kinases, including Src kinase (Aly *et al.*, 2008), and it is an agonist of the Farnesoid X receptor, a member of the nuclear receptor subfamily (Zheng *et al.*, 2017).

Recent pre-clinical studies have implicated nSMases in neurodegenerative disorders and as regulators of neuroinflammation. A recent study in an animal model of AD suggested that nSMase2 may contribute to the progression of the disease, and that nSMase2 loss of function improves neurocognitive function (Dinkins *et al.*, 2016) and limits pathological changes. Pharmacological inhibition of nSMases with Altenusin also inhibits aggregation of tau protein *in vitro* (Chua *et al.*, 2017). Gene expression of a mitochondrial-associated sphingolipid-metabolizing enzymes was shown to increase significantly in the brain of TBI mice (Novgorodov *et al.*, 2014). Another study reported the activation of the nSMase2/ceramide pathway in astrocytes, but not neurons, in the hippocampus after cerebral ischemia in rats (Gu *et al.*, 2013). nSMases appear to regulate leukocyte migration to the brain following IL-1β-induced brain injury, and their pharmacological inhibition by intrastriatal administration of Altenusin significantly reduced glial cell activation and cytokine expression (Dickens *et al.*, 2017). Furthermore, GW4869 significantly down-regulates the gene expression of pro-inflammatory cytokines (TNFα, IL-1β, IL-6) in rat hippocampus after cerebral ischemia (Gu *et al.*, 2013). Notably, GW4869 suppressed the production of pro-inflammatory cytokines in LPS-stimulated RAW264.7 macrophages, and in a sepsis induced inflammatory model (Essandoh *et al.*, 2015). Furthermore, mature dendritic cells, upon LPS stimulation, can produce pro-inflammatory cytokines, including TNF-α contained exosomes, that are attenuated by GW4869 (Gao *et al.*, 2016).

In previously published studies we demonstrated that secondary neurodegeneration and chronic neurologic deficits following experimental TBI are driven by a pronounced pro-inflammatory and neurotoxic microglial activation that persists in injured cortex for days, weeks or potentially months to years following the initial traumatic event (Byrnes *et al.*, 2012; Loane *et al.*, 2014; Loane *et al.*, 2014; Kumar *et al.*, 2016; Kumar *et al.*, 2016). We have also shown that LPS stimulation of BV2 microglia and primary microglia represent excellent *in vitro* model that mimic the pro-inflammatory neuroinflammatory events initiated acutely in our TBI model (Loane *et al.*, 2009, 2013). Using an LPS model of microglial activation *in vitro*, we demonstrate that both Altenusin and GW4869 treatment attenuate the gene expression of TNFα, IL-1β, IL-6, iNOS, and CCL2. A previous study has shown that nSMase2 is activated by TNF-α (Clarke *et al.*, 2011). Thus, our data are consistent with others indicating that nSMase2 activation is an important step for the amplification (positive feedback) of the neuroinflammatory signaling program. We investigated the effects of nSMase inhibition on the gene expression of anti-inflammatory cytokine IL-10 in activated microglia. We found that although transcriptional levels of IL-10 increased somewhat following altenusin and GW4869 pre-treatment, such changes did not reach statistical significance. These preliminary results indicate that nSMase inhibition produces robust anti-inflammatory response in microglia without upregulating inflammation-resolving programs driven by IL-10. Further investigation into mechanisms by which nSMase inhibition regulates pro- and anti-inflammatory microglial activation phenotypes will be required to identify signal transduction pathways leading to beneficial inflammation-resolving responses in microglia.

Accumulating evidence supports the involvement of miRNAs as key regulators in the pathogenesis of various neurological conditions, including neuroinflammation (Guedes *et al.*, 2013), neurodegeneration (Sabirzhanov *et al.*, 2018), autoimmune diseases (Ponomarev *et al.*,

2011), and CNS injury (Sabirzhanov *et al.*, 2014). miR-155 and miR-146 are two well-characterized pro-inflammatory miRs that are associated with microglial activation and regulate cytokine release, chemokine production, and oxidative stress (Cardoso *et al.*, 2012; Saba *et al.*, 2012, Saba *et al.*, 2014; Guedes *et al.*, 2014; Butovsky *et al.*, 2015). Prior work has shown that miR-155 and miR-146 may be involved in modulation of microglial-mediated neuroinflammation by inducing proinflammatory cytokines in microglia (Jayadev *et al.*, 2013; Yin *et al.*, 2017) and neuronal cell death in various brain injury models (Caballero-Garrido *et al.*, 2015; Harrison *et al.*, 2016, 2017; Pena-Philippides *et al.*, 2016). It has been demonstrated that miRNA-155 and -146a mediate cell-to-cell communication through exosomes/microvesicles and participate in target gene modulation in bone marrow-derived dendritic cells and cardiovascular disease (Montecalvo *et al.*, 2012; Hulsmans and Holvoet, 2013). We have recently shown that miR-155 is significantly up-regulated in cortex after experimental TBI and that central administration of miR-155 inhibitors (antagomirs) can reduce neuroinflammation and improve outcomes (Henry *et al.*, 2018). In the present study, up-regulation of miR-155 and miR-146 expression were observed in LPS-activated BV2 microglial cells. Following treatment with Altenusin or GW4869, expression of miR-155 was substantially decreased, whereas no changes were observed in miR-146 expression, providing evidence that nSMase2 acts up-stream of the key pro-inflammatory miR-155.

We, and others, have previously shown that microglia can release EVs that further activate the neighboring microglia and propagate the neuroinflammatory responses in the injured brain (Brites and Fernandes, 2015; Kumar *et al.*, 2017; Paolicelli *et al.*, 2018; Yang *et al.*, 2018). The nSMase pathway is known to be involved in the biogenesis of EVs (Menck *et al.*, 2017). Studies have shown that LPS-induced systemic inflammation causes the choroid plexus to secrete exosome and propagate a pro-inflammatory response in the brain, and that these processes can be attenuated

by GW4869 (Balusu *et al.*, 2016). LPS also enhances exosome release from pulmonary artery smooth muscle cells (PAEC), promoting cell proliferation and apoptosis resistance and contributing to the pathogenesis of pulmonary hypertension (PH); GW4869 may attenuate PH by inhibiting the exosome release (Zhao *et al.*, 2017). Inhibition of nSMase with Altenusin resulted in sharp decline in the IL-1β induced EVs *in vitro* and *in vivo* (Dickens *et al.*, 2017). The ATP receptor P2X7 and its agonists have been implicated in the shedding of IL-1β-containing MP (Bianco *et al.*, 2009; Li *et al.*, 2017) and release of proinflammatory mediators during CNS inflammatory events (Hide *et al.*, 2000; Shieh *et al.*, 2014), and that these mechanisms require acid sphingomyelinase (Bianco *et al.*, 2009). Here we examine the effect on nSMase inhibition on microglial pro-inflammatory responses and how it relates to microglial-mediated MP release. Previously, we demonstrated that MP loaded with pro-inflammatory molecules (TNFα, IL-1β, miR-155) initially released by microglia immediately following brain trauma can seed microglial-mediated neuroinflammation that may contribute to progressive neurodegeneration in the injured brain (Kumar *et al.*, 2017). In the present study we examined the effects of nSMase inhibition on MP release from microglia as an outcome measure because these drugs have previously been found to modulate release of extracellular vesicles (Essandoh *et al.*, 2015; Dickens *et al.*, 2017). We determined that nSMase inhibitors reduced the release of MP following treatment with LPS and BzATP, with Altenusin being more effective than GW4869. Thus, our data suggest that nSMases may play an important role in EVs/MP shedding in microglial and associated inflammatory responses, but further in-depth investigations are needed to determine the mechanisms involved.

Both MAPKs and NF-κB play key roles in the regulation of transcriptional activity of pro-inflammatory genes in microglia (Kim and Choi, 2010; Bachstetter *et al.*, 2011; Kopitar-Jerala, 2015; Shih *et al.*, 2015). The major MAPK pathway subfamilies involved in the regulation of

cytokines in LPS-activated microglia include signaling proteins such as p38 MAPK, extracellular signal-regulated kinase (ERK1/2) and c-jun-N terminal kinase (JNK), and NF-κB (Singh *et al.*, 2014; Kumar *et al.*, 2015; Velagapudi *et al.*, 2017). p38 MAPK is involved in the ATP-induced MP shedding and cytokine release in glial cultures (Bianco *et al.*, 2009), and has been shown to act as an up-stream regulator of nSMase2 (Clarke *et al.*, 2007; Filosto *et al.*, 2010). Here, altenusin treatment significantly reduced LPS-induced phosphorylation of p38 and ERK1/2 but had no effect on JNK phosphorylation. Stimulation of microglia with LPS also leads to IκB degradation, facilitating the translocation of NF-κB to the nucleus and subsequent transcription of proinflammatory cytokines (Olajide *et al.*, 2014). In contrast to p38/ERK MAPK, we did not observe any significant changes in the levels of IκBα following altenusin treatment, suggesting that the anti-inflammatory effects may involve attenuation of nSMases-dependent activation of specific pro-inflammatory MAPK pathways. Our data indicate that the anti-inflammatory effects exerted by altenusin may involve p38 and ERK1/2 signaling pathways, but not the JNK and NF-κB pathways.

A major driver of the neurotoxic microglial activation phenotype is NADPH oxidase (NOX2), an enzyme system highly expressed on phagocytes that produces reactive oxygen species and regulates pro-inflammatory activation pathways through NF-κB-dependent pathways (Gao *et al.*, 2012). In prior studies we demonstrated that TBI up-regulated NADPH oxidase subunits $p22^{phox}$ and NOX2 in reactive microglia in the injured cortex and that NOX2 was highly expressed in CD68/Iba1-positive microglia at 1year post-injury (Loane *et al.*, 2014). Furthermore, NOX2 deficiency reduces pro-inflammatory activation of microglia following TBI (Kumar *et al.*, 2016). These findings indicate that NOX2 contributes to pro-inflammatory microglial activation and release of neurotoxic mediators following TBI. In the current study we demonstrate the effect of

nSMase inhibition on the expression of NADPH oxidase subunit gene expression (NOX2, $p22^{phox}$) and pro-inflammatory gene expression following TBI, indicating that this important neurotoxic microglial activation pathway is inhibited by nSMase inhibitors. Notably, systemic administration of altenusin immediately following TBI significantly decreased the expression of pro-inflammatory and reactive microglial markers TNFα, IL-6, IL-1β, iNOS, CCL2, CD68, NOX2 and $p22^{phox}$ in the injured cortex of mice.

Microglia are not only pro-inflammatory or neurotoxic but also produce anti-inflammatory cytokines, alternative activation markers, and neurotrophic factors that can have positive and beneficial functions in resolving inflammation (Loane and Kumar, 2016). To address the effect of effects of altenusin on these programs we examined the gene expression of anti-inflammatory cytokines and alternative activation markers (IL-10, IL-4ra, Arg-1, Mrc1, and Ym1) in the injured cortex at 24 hours post-injury. Our results indicate that altenusin reduces pro-inflammatory responses in the injured brain without up-regulating anti-inflammatory and alternative activation pathways. Given altenusin's ability to attenuate early inflammatory events, it may be effective in improving long-term neurobehavioral and neuropathological outcomes after TBI. A challenge for the therapeutic application of nSMase inhibitors is that inhibition of nSMase2 may cause memory impairment (Tabatadze *et al.*, 2010) and motor deficits (Tan *et al.*, 2018). However, when examined in the context of AD-associated pathology, genetic nSMase2 deficiency improved cognition (Dinkins *et al.*, 2016) suggesting that in conditions where nSMases play a key role for the development of the pathological process their inhibition may, on balance, have significant therapeutic value.

Together, our studies underscore the anti-inflammatory effects of selective nSMase inhibition following experimental TBI and their potential as therapeutic target after head injury.

Further investigation is warranted to elucidate the effects of nSMase inhibitors, particularly altenusin, on behavioral outcomes following brain trauma.

Acknowledgement: We thank Ming Yang, Victoria Meadows, and Niaz Khan for their excellent technical assistance. The authors are grateful to Prof. Stephen R. Thom (University of Maryland Baltimore) for providing us the access to use flow cytometer instrument.

Authorship Contributions

Participated in research design: Kumar, Stoica, Loane

Conducted experiments: Kumar, Henry, Bhat, Abulwerdi

Performed data analysis: Kumar

Wrote or contributed to the writing of the manuscript: Kumar, Stoica, Loane, Faden

References

Aly AH, Edrada-Ebel R, Indriani ID, Wray V, Müller WEG, Totzke F, Zirrgiebel U, Schächtele C, Kubbutat MHG, Lin WH, Proksch P, and Ebel R (2008) Cytotoxic metabolites from the fungal endophyte Alternaria sp. and their subsequent detection in its host plant Polygonum senegalense. *J Nat Prod* **71**:972–980.

Bachstetter AD, Xing B, de Almeida L, Dimayuga ER, Watterson DM, and Van Eldik LJ (2011) Microglial p38α MAPK is a key regulator of proinflammatory cytokine up-regulation induced by toll-like receptor (TLR) ligands or beta-amyloid (Aβ). *J Neuroinflammation* **8**:79.

Balusu S, Van Wonterghem E, De Rycke R, Raemdonck K, Stremersch S, Gevaert K, Brkic M, Demeestere D, Vanhooren V, Hendrix A, Libert C, and Vandenbroucke RE (2016) Identification of a novel mechanism of blood-brain communication during peripheral inflammation via choroid plexus-derived extracellular vesicles. *EMBO Mol Med* **8**:1162–1183.

Beneventano M, Spampinato SF, Merlo S, Chisari M, Platania P, Ragusa M, Purrello M, Nicoletti F, and Sortino MA (2017) Shedding of Microvesicles from Microglia Contributes to the Effects Induced by Metabotropic Glutamate Receptor 5 Activation on Neuronal Death. *Front Pharmacol* **8**:812.

Bianco F, Perrotta C, Novellino L, Francolini M, Riganti L, Menna E, Saglietti L, Schuchman EH, Furlan R, Clementi E, Matteoli M, and Verderio C (2009) Acid sphingomyelinase activity triggers microparticle release from glial cells. *EMBO J* **28**:1043–1054.

Bianco F, Pravettoni E, Colombo A, Schenk U, Möller T, Matteoli M, and Verderio C (2005) Astrocyte-derived ATP induces vesicle shedding and IL-1 beta release from microglia. *J Immunol* **174**:7268–7277.

Bilousova T, Elias C, Miyoshi E, Alam MP, Zhu C, Campagna J, Vadivel K, Jagodzinska B, Gylys KH, and John V (2018) Suppression of tau propagation using an inhibitor that targets the DK-switch of nSMase2. *Biochem Biophys Res Commun* **499**:751–757.

Bohman L-E, Riley J, Milovanova TN, Sanborn MR, Thom SR, and Armstead WM (2016) Microparticles Impair Hypotensive Cerebrovasodilation and Cause Hippocampal Neuronal Cell Injury after Traumatic Brain Injury. *J Neurotrauma* **33**:168–174.

Brann AB, Tcherpakov M, Williams IM, Futerman AH, and Fainzilber M (2002) Nerve growth factor-induced p75-mediated death of cultured hippocampal neurons is age-dependent and transduced through ceramide generated by neutral sphingomyelinase. *J Biol Chem* **277**:9812–9818.

Brites D, and Fernandes A (2015) Neuroinflammation and Depression: Microglia Activation, Extracellular Microvesicles and microRNA Dysregulation. *Frontiers in Cellular Neuroscience* **9**.

Butovsky O, Jedrychowski MP, Cialic R, Krasemann S, Murugaiyan G, Fanek Z, Greco DJ, Wu PM, Doykan CE, Kiner O, Lawson RJ, Frosch MP, Pochet N, Fatimy RE, Krichevsky AM, Gygi SP, Lassmann H, Berry J, Cudkowicz ME, and Weiner HL (2015) Targeting miR-155 restores abnormal microglia and attenuates disease in SOD1 mice. *Ann Neurol* **77**:75–99.

Byrnes KR, Loane DJ, Stoica BA, Zhang J, and Faden AI (2012) Delayed mGluR5 activation limits neuroinflammation and neurodegeneration after traumatic brain injury. *J Neuroinflammation* **9**:43.

Caballero-Garrido E, Pena-Philippides JC, Lordkipanidze T, Bragin D, Yang Y, Erhardt EB, and Roitbak T (2015) In Vivo Inhibition of miR-155 Promotes Recovery after Experimental Mouse Stroke. *J Neurosci* **35**:12446–12464.

Cardoso AL, Guedes JR, Pereira de Almeida L, and Pedroso de Lima MC (2012) miR-155 modulates microglia-mediated immune response by down-regulating SOCS-1 and promoting cytokine and nitric oxide production. *Immunology* **135**:73–88.

Chua SW, Cornejo A, van Eersel J, Stevens CH, Vaca I, Cueto M, Kassiou M, Gladbach A, Macmillan A, Lewis L, Whan R, and Ittner LM (2017) The Polyphenol Altenusin Inhibits in Vitro Fibrillization of Tau and Reduces Induced Tau Pathology in Primary Neurons. *ACS Chem Neurosci* **8**:743–751.

Clarke CJ, Cloessner EA, Roddy PL, and Hannun YA (2011) Neutral sphingomyelinase 2 (nSMase2) is the primary neutral sphingomyelinase isoform activated by tumour necrosis factor-α in MCF-7 cells. *Biochem J* **435**:381–390.

Clarke CJ, Truong T-G, and Hannun YA (2007) Role for Neutral Sphingomyelinase-2 in Tumor Necrosis Factor α-Stimulated Expression of Vascular Cell Adhesion Molecule-1 (VCAM) and Intercellular Adhesion Molecule-1 (ICAM) in Lung Epithelial Cells: p38 MAPK IS AN UPSTREAM REGULATOR OF nSMase2. *Journal of Biological Chemistry* **282**:1384–1396.

Dickens AM, Tovar-Y-Romo LB, Yoo S-W, Trout AL, Bae M, Kanmogne M, Megra B, Williams DW, Witwer KW, Gacias M, Tabatadze N, Cole RN, Casaccia P, Berman JW, Anthony

DC, and Haughey NJ (2017) Astrocyte-shed extracellular vesicles regulate the peripheral leukocyte response to inflammatory brain lesions. *Sci Signal* **10**.

Dinkins MB, Enasko J, Hernandez C, Wang G, Kong J, Helwa I, Liu Y, Terry AV, and Bieberich E (2016) Neutral Sphingomyelinase-2 Deficiency Ameliorates Alzheimer's Disease Pathology and Improves Cognition in the 5XFAD Mouse. *J Neurosci* **36**:8653–8667.

Erdbruegger (2010) Detection of circulating microparticles by flow cytometry: influence of centrifugation, filtration of buffer, and freezing. *Vascular Health and Risk Management* 1125.

Essandoh K, Yang L, Wang X, Huang W, Qin D, Hao J, Wang Y, Zingarelli B, Peng T, and Fan G-C (2015) Blockade of exosome generation with GW4869 dampens the sepsis-induced inflammation and cardiac dysfunction. *Biochim Biophys Acta* **1852**:2362–2371.

Fenn AM, Gensel JC, Huang Y, Popovich PG, Lifshitz J, and Godbout JP (2014) Immune activation promotes depression 1 month after diffuse brain injury: a role for primed microglia. *Biol Psychiatry* **76**:575–584.

Figuera-Losada M, Stathis M, Dorskind JM, Thomas AG, Bandaru VVR, Yoo S-W, Westwood NJ, Rogers GW, McArthur JC, Haughey NJ, Slusher BS, and Rojas C (2015) Cambinol, a Novel Inhibitor of Neutral Sphingomyelinase 2 Shows Neuroprotective Properties. *PLOS ONE* **10**:e0124481.

Filosto S, Fry W, Knowlton AA, and Goldkorn T (2010) Neutral Sphingomyelinase 2 (nSMase2) Is a Phosphoprotein Regulated by Calcineurin (PP2B). *Journal of Biological Chemistry* **285**:10213–10222.

Fu R, Shen Q, Xu P, Luo JJ, and Tang Y (2014) Phagocytosis of microglia in the central nervous system diseases. *Mol Neurobiol* **49**:1422–1434.

Gao H-M, Zhou H, and Hong J-S (2012) NADPH oxidases: novel therapeutic targets for neurodegenerative diseases. *Trends Pharmacol Sci* **33**:295–303.

Gao W, Liu H, Yuan J, Wu C, Huang D, Ma Y, Zhu J, Ma L, Guo J, Shi H, Zou Y, and Ge J (2016) Exosomes derived from mature dendritic cells increase endothelial inflammation and atherosclerosis via membrane TNF-α mediated NF-κB pathway. *J Cell Mol Med* **20**:2318–2327.

Gu L, Huang B, Shen W, Gao L, Ding Z, Wu H, and Guo J (2013) Early activation of nSMase2/ceramide pathway in astrocytes is involved in ischemia-associated neuronal damage via inflammation in rat hippocampi. *J Neuroinflammation* **10**:109.

Guedes J, Cardoso ALC, and Pedroso de Lima MC (2013) Involvement of MicroRNA in Microglia-Mediated Immune Response. *Clinical and Developmental Immunology* **2013**:1–11.

Guedes JR, Custódia CM, Silva RJ, de Almeida LP, Pedroso de Lima MC, and Cardoso AL (2014) Early miR-155 upregulation contributes to neuroinflammation in Alzheimer's disease triple transgenic mouse model. *Hum Mol Genet* **23**:6286–6301.

Guo BB, Bellingham SA, and Hill AF (2015) The neutral sphingomyelinase pathway regulates packaging of the prion protein into exosomes. *J Biol Chem* **290**:3455–3467.

Hanisch U-K (2002) Microglia as a source and target of cytokines. *Glia* **40**:140–155.

Harrison EB, Emanuel K, Lamberty BG, Morsey BM, Li M, Kelso ML, Yelamanchili SV, and Fox HS (2017) Induction of miR-155 after Brain Injury Promotes Type 1 Interferon and has a Neuroprotective Effect. *Frontiers in Molecular Neuroscience* **10**.

Harrison EB, Hochfelder CG, Lamberty BG, Meays BM, Morsey BM, Kelso ML, Fox HS, and Yelamanchili SV (2016) Traumatic brain injury increases levels of miR-21 in extracellular vesicles: implications for neuroinflammation. *FEBS Open Bio* **6**:835–846.

Harrison-Brown M, Liu G-J, and Banati R (2016) Checkpoints to the Brain: Directing Myeloid Cell Migration to the Central Nervous System. *Int J Mol Sci* **17**.

Hazelton I, Yates A, Dale A, Roodselaar J, Akbar N, Ruitenberg MJ, Anthony DC, and Couch Y (2018) Exacerbation of Acute Traumatic Brain Injury by Circulating Extracellular Vesicles. *J Neurotrauma* **35**:639–651.

Henry RJ, Doran SJ, Barrett JP, Meadows VE, Sabirzhanov B, Stoica BA, Loane DJ, and Faden AI (2018) Inhibition of miR-155 Limits Neuroinflammation and Improves Functional Recovery After Experimental Traumatic Brain Injury in Mice. *Neurotherapeutics*, doi: 10.1007/s13311-018-0665-9.

Hide I, Tanaka M, Inoue A, Nakajima K, Kohsaka S, Inoue K, and Nakata Y (2000) Extracellular ATP triggers tumor necrosis factor-alpha release from rat microglia. *J Neurochem* **75**:965–972.

Huang Y, Li Y, Zhang H, Zhao R, Jing R, Xu Y, He M, Peer J, Kim YC, Luo J, Tong Z, and Zheng J (2018) Zika virus propagation and release in human fetal astrocytes can be suppressed by neutral sphingomyelinase-2 inhibitor GW4869. *Cell Discov* **4**:19.

Hulsmans M, and Holvoet P (2013) MicroRNA-containing microvesicles regulating inflammation in association with atherosclerotic disease. *Cardiovascular Research* **100**:7–18.

Hung T-H, Shyue S-K, Wu C-H, Chen C-C, Lin C-C, Chang C-F, and Chen S-F (2017) Deletion or inhibition of soluble epoxide hydrolase protects against brain damage and reduces

microglia-mediated neuroinflammation in traumatic brain injury. *Oncotarget* **8**:103236–103260.

Iguchi Y, Eid L, Parent M, Soucy G, Bareil C, Riku Y, Kawai K, Takagi S, Yoshida M, Katsuno M, Sobue G, and Julien J-P (2016) Exosome secretion is a key pathway for clearance of pathological TDP-43. *Brain* **139**:3187–3201.

Jayadev S, Case A, Alajajian B, Eastman AJ, Möller T, and Garden GA (2013) Presenilin 2 influences miR146 level and activity in microglia. *J Neurochem* **127**:592–599.

Kabadi SV, Stoica BA, Hanscom M, Loane DJ, Kharebava G, Murray Ii MG, Cabatbat RM, and Faden AI (2012) CR8, a selective and potent CDK inhibitor, provides neuroprotection in experimental traumatic brain injury. *Neurotherapeutics* **9**:405–421.

Kaminska B (2005) MAPK signalling pathways as molecular targets for anti-inflammatory therapy--from molecular mechanisms to therapeutic benefits. *Biochim Biophys Acta* **1754**:253–262.

Kaminska B, Gozdz A, Zawadzka M, Ellert-Miklaszewska A, and Lipko M (2009) MAPK signal transduction underlying brain inflammation and gliosis as therapeutic target. *Anat Rec (Hoboken)* **292**:1902–1913.

Kim EK, and Choi E-J (2010) Pathological roles of MAPK signaling pathways in human diseases. *Biochimica et Biophysica Acta (BBA) - Molecular Basis of Disease* **1802**:396–405.

Kopitar-Jerala N (2015) Innate Immune Response in Brain, NF-Kappa B Signaling and Cystatins. *Frontiers in Molecular Neuroscience* **8**.

Kumar A, Alvarez-Croda D-M, Stoica BA, Faden AI, and Loane DJ (2016) Microglial/Macrophage Polarization Dynamics following Traumatic Brain Injury. *J Neurotrauma* **33**:1732–1750.

Kumar A, Barrett JP, Alvarez-Croda D-M, Stoica BA, Faden AI, and Loane DJ (2016) NOX2 drives M1-like microglial/macrophage activation and neurodegeneration following experimental traumatic brain injury. *Brain Behav Immun* **58**:291–309.

Kumar A, Bhatia HS, de Oliveira ACP, and Fiebich BL (2015) microRNA-26a modulates inflammatory response induced by toll-like receptor 4 stimulation in microglia. *J Neurochem*, doi: 10.1111/jnc.13364.

Kumar Alok, Stoica BA, Loane DJ, Yang M, Abulwerdi G, Khan N, Kumar Asit, Thom SR, and Faden AI (2017) Microglial-derived microparticles mediate neuroinflammation after traumatic brain injury. *J Neuroinflammation* **14**:47.

Lee J-T, Xu J, Lee J-M, Ku G, Han X, Yang D-I, Chen S, and Hsu CY (2004) Amyloid-beta peptide induces oligodendrocyte death by activating the neutral sphingomyelinase-ceramide pathway. *J Cell Biol* **164**:123–131.

Li J, Li X, Jiang X, Yang M, Yang R, Burnstock G, Xiang Z, and Yuan H (2017) Microvesicles shed from microglia activated by the P2X7-p38 pathway are involved in neuropathic pain induced by spinal nerve ligation in rats. *Purinergic Signal* **13**:13–26.

Livak KJ, and Schmittgen TD (2001) Analysis of Relative Gene Expression Data Using Real-Time Quantitative PCR and the 2−ΔΔCT Method. *Methods* **25**:402–408.

Loane DJ, and Byrnes KR (2010) Role of microglia in neurotrauma. *Neurotherapeutics* **7**:366–377.

Loane DJ, and Kumar A (2016) Microglia in the TBI brain: The good, the bad, and the dysregulated. *Exp Neurol* **275 Pt 3**:316–327.

Loane DJ, Kumar A, Stoica BA, Cabatbat R, and Faden AI (2014) Progressive neurodegeneration after experimental brain trauma: association with chronic microglial activation. *J Neuropathol Exp Neurol* **73**:14–29.

Loane DJ, Stoica BA, Byrnes KR, Jeong W, and Faden AI (2013) Activation of mGluR5 and inhibition of NADPH oxidase improves functional recovery after traumatic brain injury. *J Neurotrauma* **30**:403–412.

Loane DJ, Stoica BA, Pajoohesh-Ganji A, Byrnes KR, and Faden AI (2009) Activation of metabotropic glutamate receptor 5 modulates microglial reactivity and neurotoxicity by inhibiting NADPH oxidase. *J Biol Chem* **284**:15629–15639.

Loane DJ, Stoica BA, Tchantchou F, Kumar A, Barrett JP, Akintola T, Xue F, Conn PJ, and Faden AI (2014) Novel mGluR5 Positive Allosteric Modulator Improves Functional Recovery, Attenuates Neurodegeneration, and Alters Microglial Polarization after Experimental Traumatic Brain Injury. *Neurotherapeutics* **11**:857–869.

Luberto C, Hassler DF, Signorelli P, Okamoto Y, Sawai H, Boros E, Hazen-Martin DJ, Obeid LM, Hannun YA, and Smith GK (2002) Inhibition of tumor necrosis factor-induced cell death in MCF7 by a novel inhibitor of neutral sphingomyelinase. *J Biol Chem* **277**:41128–41139.

Mao S-S, Hua R, Zhao X-P, Qin X, Sun Z-Q, Zhang Y, Wu Y-Q, Jia M-X, Cao J-L, and Zhang Y-M (2012) Exogenous administration of PACAP alleviates traumatic brain injury in rats through a mechanism involving the TLR4/MyD88/NF-κB pathway. *J Neurotrauma* **29**:1941–1959.

Martinez TN, Chen X, Bandyopadhyay S, Merrill AH, and Tansey MG (2012) Ceramide sphingolipid signaling mediates Tumor Necrosis Factor (TNF)-dependent toxicity via caspase signaling in dopaminergic neurons. *Mol Neurodegener* **7**:45.

Menck K, Sönmezer C, Worst TS, Schulz M, Dihazi GH, Streit F, Erdmann G, Kling S, Boutros M, Binder C, and Gross JC (2017) Neutral sphingomyelinases control extracellular vesicles budding from the plasma membrane. *J Extracell Vesicles* **6**:1378056.

Montecalvo A, Larregina AT, Shufesky WJ, Stolz DB, Sullivan MLG, Karlsson JM, Baty CJ, Gibson GA, Erdos G, Wang Z, Milosevic J, Tkacheva OA, Divito SJ, Jordan R, Lyons-Weiler J, Watkins SC, and Morelli AE (2012) Mechanism of transfer of functional microRNAs between mouse dendritic cells via exosomes. *Blood* **119**:756–766.

Mosmann T (1983) Rapid colorimetric assay for cellular growth and survival: application to proliferation and cytotoxicity assays. *J Immunol Methods* **65**:55–63.

Nigro A, Colombo F, Casella G, Finardi A, Verderio C, and Furlan R (2016) Myeloid Extracellular Vesicles: Messengers from the Demented Brain. *Front Immunol* **7**:17.

Novgorodov SA, Riley CL, Yu J, Borg KT, Hannun YA, Proia RL, Kindy MS, and Gudz TI (2014) Essential roles of neutral ceramidase and sphingosine in mitochondrial dysfunction due to traumatic brain injury. *J Biol Chem* **289**:13142–13154.

Olajide OA, Kumar A, Velagapudi R, Okorji UP, and Fiebich BL (2014) Punicalagin inhibits neuroinflammation in LPS-activated rat primary microglia. *Molecular Nutrition & Food Research* **58**:1843–1851.

Paolicelli RC, Bergamini G, and Rajendran L (2018) Cell-to-cell Communication by Extracellular Vesicles: Focus on Microglia. *Neuroscience*, doi: 10.1016/j.neuroscience.2018.04.003.

Pena-Philippides JC, Caballero-Garrido E, Lordkipanidze T, and Roitbak T (2016) In vivo inhibition of miR-155 significantly alters post-stroke inflammatory response. *Journal of Neuroinflammation* **13**.

Perry VH, Nicoll JAR, and Holmes C (2010) Microglia in neurodegenerative disease. *Nat Rev Neurol* **6**:193–201.

Pieragostino D, Cicalini I, Lanuti P, Ercolino E, di Ioia M, Zucchelli M, Zappacosta R, Miscia S, Marchisio M, Sacchetta P, Onofrj M, and Del Boccio P (2018) Enhanced release of acid sphingomyelinase-enriched exosomes generates a lipidomics signature in CSF of Multiple Sclerosis patients. *Sci Rep* **8**:3071.

Poncelet P, Robert S, Bailly N, Garnache-Ottou F, Bouriche T, Devalet B, Segatchian JH, Saas P, and Mullier F (2015) Tips and tricks for flow cytometry-based analysis and counting of microparticles. *Transfusion and Apheresis Science* **53**:110–126.

Ponomarev ED, Veremeyko T, Barteneva N, Krichevsky AM, and Weiner HL (2011) MicroRNA-124 promotes microglia quiescence and suppresses EAE by deactivating macrophages via the C/EBP-α-PU.1 pathway. *Nat Med* **17**:64–70.

Prinz M, and Priller J (2014) Microglia and brain macrophages in the molecular age: from origin to neuropsychiatric disease. *Nature Reviews Neuroscience* **15**:300–312.

Saba R, Gushue S, Huzarewich RLCH, Manguiat K, Medina S, Robertson C, and Booth SA (2012) MicroRNA 146a (miR-146a) is over-expressed during prion disease and modulates the innate immune response and the microglial activation state. *PLoS ONE* **7**:e30832.

Saba R, Sorensen DL, and Booth SA (2014) MicroRNA-146a: A Dominant, Negative Regulator of the Innate Immune Response. *Front Immunol* **5**:578.

Sabirzhanov B, Faden AI, Aubrecht T, Henry R, Glaser E, and Stoica BA (2018) MicroRNA-711-Induced Downregulation of Angiopoietin-1 Mediates Neuronal Cell Death. *J Neurotrauma*, doi: 10.1089/neu.2017.5572.

Sabirzhanov B, Zhao Z, Stoica BA, Loane DJ, Wu J, Borroto C, Dorsey SG, and Faden AI (2014) Downregulation of miR-23a and miR-27a following experimental traumatic brain injury induces neuronal cell death through activation of proapoptotic Bcl-2 proteins. *J Neurosci* **34**:10055–10071.

Shet AS, Key NS, and Hebbel RP (2004) Measuring circulating cell-derived microparticles. *Journal of Thrombosis and Haemostasis* **2**:1848–1850.

Shieh C-H, Heinrich A, Serchov T, van Calker D, and Biber K (2014) P2X7-dependent, but differentially regulated release of IL-6, CCL2, and TNF-α in cultured mouse microglia. *Glia* **62**:592–607.

Shih R-H, Wang C-Y, and Yang C-M (2015) NF-kappaB Signaling Pathways in Neurological Inflammation: A Mini Review. *Front Mol Neurosci* **8**:77.

Singh V, Bhatia HS, Kumar A, de Oliveira ACP, and Fiebich BL (2014) Histone deacetylase inhibitors valproic acid and sodium butyrate enhance prostaglandins release in lipopolysaccharide-activated primary microglia. *Neuroscience* **265**:147–157.

Sobue A, Ito N, Nagai T, Shan W, Hada K, Nakajima A, Murakami Y, Mouri A, Yamamoto Y, Nabeshima T, Saito K, and Yamada K (2018) Astroglial major histocompatibility complex class I following immune activation leads to behavioral and neuropathological changes. *Glia* **66**:1034–1052.

Song L, Lee C, and Schindler C (2011) Deletion of the murine scavenger receptor CD68. *J Lipid Res* **52**:1542–1550.

Stoica BA, Loane DJ, Zhao Z, Kabadi SV, Hanscom M, Byrnes KR, and Faden AI (2014) PARP-1 inhibition attenuates neuronal loss, microglia activation and neurological deficits after traumatic brain injury. *J Neurotrauma* **31**:758–772.

Tabatadze N, Savonenko A, Song H, Bandaru VVR, Chu M, and Haughey NJ (2010) Inhibition of neutral sphingomyelinase-2 perturbs brain sphingolipid balance and spatial memory in mice. *J Neurosci Res* **88**:2940–2951.

Tan LH-R, Tan AJ-R, Ng Y-Y, Chua JJ-E, Chew W-S, Muralidharan S, Torta F, Dutta B, Sze SK, Herr DR, and Ong W-Y (2018) Enriched Expression of Neutral Sphingomyelinase 2 in the Striatum is Essential for Regulation of Lipid Raft Content and Motor Coordination. *Mol Neurobiol* **55**:5741–5756.

Taylor DD, and Gercel-Taylor C (2014) Exosome platform for diagnosis and monitoring of traumatic brain injury. *Philos Trans R Soc Lond, B, Biol Sci* **369**.

Thelin EP, Tajsic T, Zeiler FA, Menon DK, Hutchinson PJA, Carpenter KLH, Morganti-Kossmann MC, and Helmy A (2017) Monitoring the Neuroinflammatory Response Following Acute Brain Injury. *Frontiers in Neurology* **8**.

Tian Y, Salsbery B, Wang M, Yuan H, Yang J, Zhao Z, Wu X, Zhang Y, Konkle BA, Thiagarajan P, Li M, Zhang J, and Dong J -f. (2015) Brain-derived microparticles induce systemic coagulation in a murine model of traumatic brain injury. *Blood* **125**:2151–2159.

Uchida R, Tomoda H, Dong Y, and Omura S (1999) Alutenusin, a specific neutral sphingomyelinase inhibitor, produced by Penicillium sp. FO-7436. *J Antibiot* **52**:572–574.

Velagapudi R, Kumar A, Bhatia HS, El-Bakoush A, Lepiarz I, Fiebich BL, and Olajide OA (2017) Inhibition of neuroinflammation by thymoquinone requires activation of Nrf2/ARE signalling. *Int Immunopharmacol* **48**:17–29.

Walker DG, and Lue L-F (2015) Immune phenotypes of microglia in human neurodegenerative disease: challenges to detecting microglial polarization in human brains. *Alzheimers Res Ther* **7**:56.

Woodcock T, and Morganti-Kossmann MC (2013) The role of markers of inflammation in traumatic brain injury. *Front Neurol* **4**:18.

Wu BX, Rajagopalan V, Roddy PL, Clarke CJ, and Hannun YA (2010) Identification and characterization of murine mitochondria-associated neutral sphingomyelinase (MA-nSMase), the mammalian sphingomyelin phosphodiesterase 5. *J Biol Chem* **285**:17993–18002.

Wu M, Harvey KA, Ruzmetov N, Welch ZR, Sech L, Jackson K, Stillwell W, Zaloga GP, and Siddiqui RA (2005) Omega-3 polyunsaturated fatty acids attenuate breast cancer growth through activation of a neutral sphingomyelinase-mediated pathway. *Int J Cancer* **117**:340–348.

Xiao C, Wang K, Xu Y, Hu H, Zhang N, Wang Y, Zhong Z, Zhao J, Li Q, Zhu D, Ke C, Zhong S, Wu X, Yu H, Zhu W, Chen J, Zhang J, Wang J, and Hu X (2018) Transplanted Mesenchymal Stem Cells Reduce Autophagic Flux in Infarcted Hearts via the Exosomal Transfer of miR-125b. *Circ Res* **123**:564–578.

Xiao T, Zhang W, Jiao B, Pan C-Z, Liu X, and Shen L (2017) The role of exosomes in the pathogenesis of Alzheimer' disease. *Transl Neurodegener* **6**:3.

Yang Y, Boza-Serrano A, Dunning CJR, Clausen BH, Lambertsen KL, and Deierborg T (2018) Inflammation leads to distinct populations of extracellular vesicles from microglia. *Journal of Neuroinflammation* **15**.

Yin H, Song S, and Pan X (2017) Knockdown of miR-155 protects microglia against LPS-induced inflammatory injury via targeting RACK1: a novel research for intracranial infection. *Journal of Inflammation* **14**.

Yuan Y, Zhu F, Pu Y, Wang D, Huang A, Hu X, Qin S, Sun X, Su Z, and He C (2015) Neuroprotective effects of nitidine against traumatic CNS injury via inhibiting microglia activation. *Brain Behav Immun* **48**:287–300.

Zeng C, Lee JT, Chen H, Chen S, Hsu CY, and Xu J (2005) Amyloid-beta peptide enhances tumor necrosis factor-alpha-induced iNOS through neutral sphingomyelinase/ceramide pathway in oligodendrocytes. *J Neurochem* **94**:703–712.

Zhao L, Luo H, Li X, Li T, He J, Qi Q, Liu Y, and Yu Z (2017) Exosomes Derived from Human Pulmonary Artery Endothelial Cells Shift the Balance between Proliferation and Apoptosis of Smooth Muscle Cells. *Cardiology* **137**:43–53.

Zheng Z, Zhao Z, Li Shuqiang, Lu X, Jiang M, Lin J, An Y, Xie Y, Xu M, Shen W, Guo GL, Huang Y, Li Song, Zhang X, and Xie W (2017) Altenusin, a Nonsteroidal Microbial Metabolite, Attenuates Nonalcoholic Fatty Liver Disease by Activating the Farnesoid X Receptor. *Mol Pharmacol* **92**:425–436.

Competing interest: The authors have no conflict of interest to declare.

Footnotes

This work was supported by the National Institutes of Health [Grant Number R01NS037313 (A.I. Faden), R01NS082308 (D.J. Loane), and R01NS096002 (B. Stoica)].

Figure legends

Fig. 1. Effects of altenusin (A) and GW4869 (B) on the viability of BV2 microglia cells. (C-D) Cells were pre-treated with altenusin (1 - 100 µM; 1C) and GW4869 (1 - 20 µM; 1D) for 30 min, afterwards cells were stimulated with or without LPS (20 ng/ml) for the next 24 h. At the end of incubation period, MTT assays were performed on the cells to assess the cell viability. All values are expressed as mean ± SEM for at least three independent experiments. Data were analyzed using one-way ANOVA for multiple comparison with post hoc Tukey's test. (*$P < 0.05$, **$P < 0.01$) as compared with control cells.

Fig. 2. Effects of altenusin and GW4869 on the expression of pro-inflammatory mediators in BV2 microglia (A-L). Cells were pre-treated with altenusin (10 - 100 µM) for 30 min, afterwards cells were stimulated with or without LPS (20 ng/ml) for 4 h for studying gene expression of TNF-α (A), IL-6 (B), IL-1β (C), iNOS (D), CCL2 (E), IL-10 (F). Similarly, for analyzing effect of GW4869 on gene expression of inflammatory mediators, cells were pretreated with GW4869 (5 – 10 µM) for 30 min followed by stimulation with or without LPS (20 ng/ml) for the next 4 h for analyzing gene expression of TNF-α (G), IL-6 (H), IL-1β (I), iNOS (J), CCL2 (K), IL-10 (L). Data are presented as percentage control of LPS. Statistical analyses were carried out by using one-way ANOVA with post hoc Tukey's test (multiple comparisons). Results are expressed as mean ± SEM of at least three independent experiments. (*$P < 0.05$, **$P < 0.01$, ***$P < 0.001$) in comparison with LPS.

Fig. 3. Effects of altenusin and GW4869 on the release of Nitrite (A, B) and TNF-α (C, D) in BV2 microglia cells. For Nitrite estimation, cells were pre-treated with altenusin (10 -100 µM; A) and GW4869 (1 – 10 µM; B). For TNF-α ELISA, cells were pre-treated with altenusin (50 - 100 µM; C) and GW4869 (5 – 10 µM; D). Cells were pre-treated for 30 min followed by stimulation with or without LPS (20 ng/ml) for the next 24 h. At the end of incubation, cell supernatants were collected; centrifuged and release of Nitrite, and TNF-α was quantified by using Griess reagent assay and mouse specific ELISA assay, respectively. Statistical analyses were carried out by using one-way ANOVA with post hoc Tukey's test (multiple comparisons). Results are expressed as mean ± SEM of at least three independent experiments. (*$P < 0.05$, **$P < 0.01$, ***$P < 0.001$) in comparison with LPS.

Fig. 4. Effects of altenusin on the expression of pro-inflammatory mediators in primary rat microglia (A-E). Cells were pre-treated with altenusin (10 - 50 µM) for 30 min, afterwards cells were stimulated with LPS (20 ng/ml) for 4 h for studying gene expression of TNF-α (A), IL-6 (B), IL-1β (C), iNOS (D), CCL2 (E). Data are presented as percentage control of LPS. Statistical analyses were carried out by using one-way ANOVA with post hoc Tukey's test (multiple comparisons). Results are expressed as mean ± SEM of at least three independent experiments. (*$P < 0.05$, **$P < 0.01$, ***$P < 0.001$) in comparison with LPS.

Fig. 5. Effects of altenusin on the release of Nitrite and TNF-α in primary rat microglia (A, B). For estimation of Nitrite and TNF-α release, cells were pre-treated with altenusin (10 - 50 µM) for 30 min followed by stimulation with LPS (20 ng/ml) for the next 24 h. At the end of incubation, cell supernatants were collected; centrifuged and release of Nitrite (A), and TNF-α (B) was

quantified by using Griess reagent assay and rat specific ELISA assay, respectively. For miRNA expression of miR-155 (C) and miR-146 (D), cells were pre-treated with altenusin (50 - 100 µM) and GW4869 (5 – 10 µM) for 30 min, followed by LPS stimulation for 4 h. Altenusin (100 µM) and GW4869 (10 µM) significantly decreased the miR-155 (C), but not miR-146 (D), expression in LPS stimulated BV2 cells. Statistical analyses were carried out by using one-way ANOVA with post hoc Tukey's test (multiple comparisons). Results are expressed as means ± SE of at least three independent experiments. (*$P < 0.05$, **$P < 0.01$, ***$P < 0.001$) in comparison with LPS.

Fig. 6. Microglia derived MP are decreased in the BV2 cell culture supernatant following treatment of altenusin and GW4869. BV2 microglial cells were pre-treated with altenusin (50 - 100 µM) and GW4869 (5 - 10 µM) for 30 min followed by LPS (20 ng/ml) stimulation for 24 h. Afterwards cells were incubated with BzATP (100 µM) for 30 min. (A) At the end of incubation, cell supernatants were collected; centrifuged and release of MPs ware quantified by flow cytometry. Flow cytometry analysis of enriched MP isolated from the supernatant using sequential centrifugation at 300xg for 10 min, 2100xg for 10 min followed by 100,000xg for 1 h. Representation of gating strategy used to characterize MP using SSC-H and standard microbeads (300 - 1000 nm diameter). Standard microbeads were used as an internal control to determine the size of MP in the supernatant, and annexin V staining confirmed MP characteristics. (B) Flow cytometric quantification. Bars represent mean ± SEM. Data represent results of at least three independent experiments. (*$P < 0.05$, **$P < 0.01$, ***$P < 0.001$) in comparison with LPS and BzATP combined.

Fig. 7. Effects of altenusin on the phosphorylation of p38, ERK 1/2, JNK, degradation of IκBα induced by LPS. BV2 cells were pre-treated with altenusin (50 - 100 μM) for 30 min followed by stimulation with LPS (20 ng/ml) for 30 min (for phospho-p38, -ERK1/2 and -JNK) and 15 min (for IκBα). Whole cell lysates were used for western blot analysis. (A) show the representative blots and densitometric analysis (B-E) of p38 MAPK (B), ERK1/2 MAPK (C), JNK (D), and IκBα (E), respectively. Statistical analyses were carried out by using one-way ANOVA with post hoc Tukey's multiple comparisons test. Results are expressed as means ± SEM of at least three independent experiments. (*$P < 0.05$, **$P < 0.01$, ***$P < 0.001$) in comparison with LPS activated cells.

Fig. 8. Systemic administration of altenusin (2 mg/kg and 10 mg/kg) at 30 minutes post-injury. Mice were euthanized and perfused after 24 h, and cortical tissue was processed for mRNA analyses (A). Gene expression of proinflammatory molecules were analyzed in the cortex of sham and vehicle and altenusin administered TBI mice (Vehicle treated CCI significantly induced expression of proinflammatory mediators, TNF-α (B), IL-6 (C), IL-1β (D), iNOS (E) CCL2 (F), and microglia activation marker CD68 (G), reactive oxygen species (ROS) inducer NOX2 (H) and p22-phox (I), compared to sham animals. Altenusin treated (10 mg/kg) significantly reduced expression of all above mentioned genes. Analysis done by one-way ANOVA, followed by post hoc adjustments using Tukey's multiple comparison test. Results are expressed as means ± SEM (N=5-7 animals each group). (*$P < 0.05$, **$P < 0.01$, ***$P < 0.001$) in comparison with TBI (vehicle).

Fig. 9. Systemic administration of altenusin (2 mg/kg and 10 mg/kg) at 30 minutes post-injury. Mice were euthanized and perfused after 24 h, and cortical tissue was processed for mRNA analyses. Gene expression of anti-inflammatory and alternative activation markers IL-10 (A), IL-4ra (B), Mrc1/CD206 (C), Arg-1 (D), and Ym1/Chil3 (E), were analyzed in the cortex of sham, vehicle and altenusin administered TBI mice. Analysis done by one-way ANOVA, followed by post hoc adjustments using Tukey's multiple comparison test. Results are expressed as means ± SEM (N=4-7 animals each group). (*$P < 0.05$, **$P < 0.01$, ***$P < 0.001$).

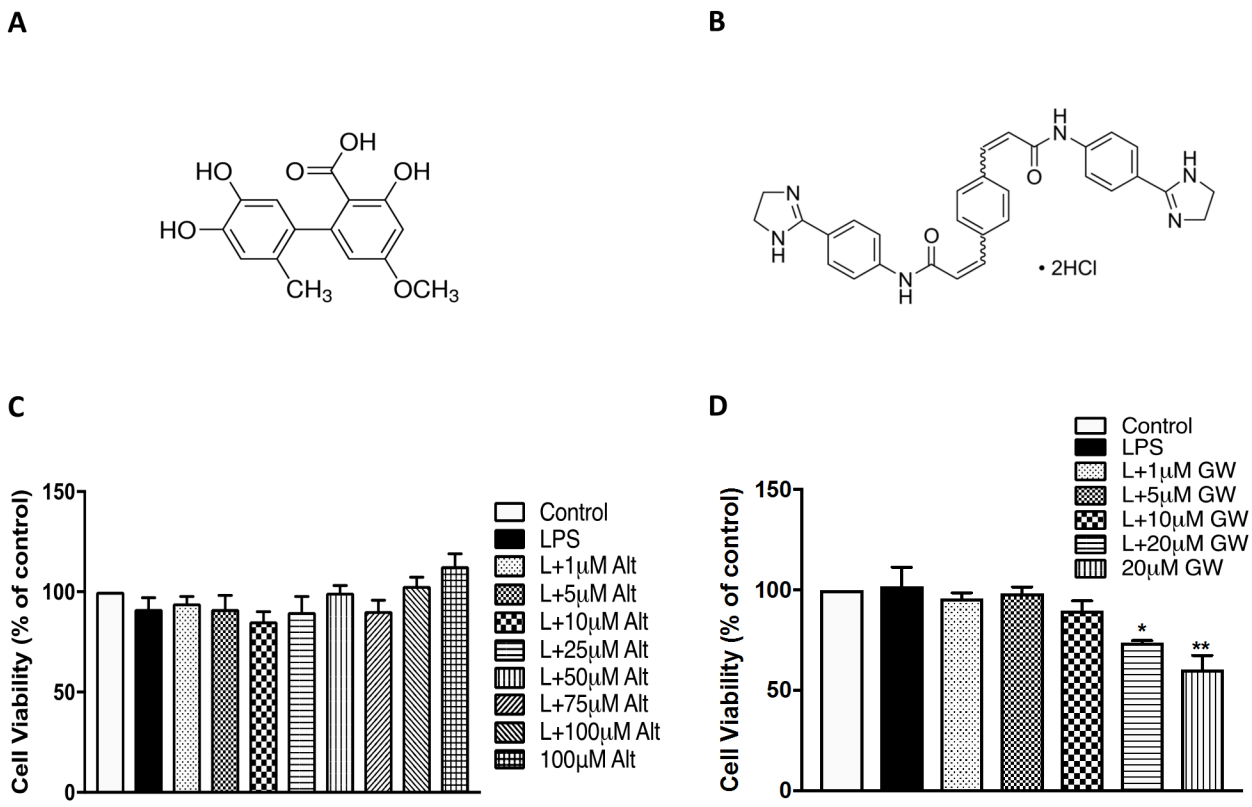

Fig. 1

JPET Fast Forward. Published on December 18, 2018 as DOI: 10.1124/jpet.118.253393

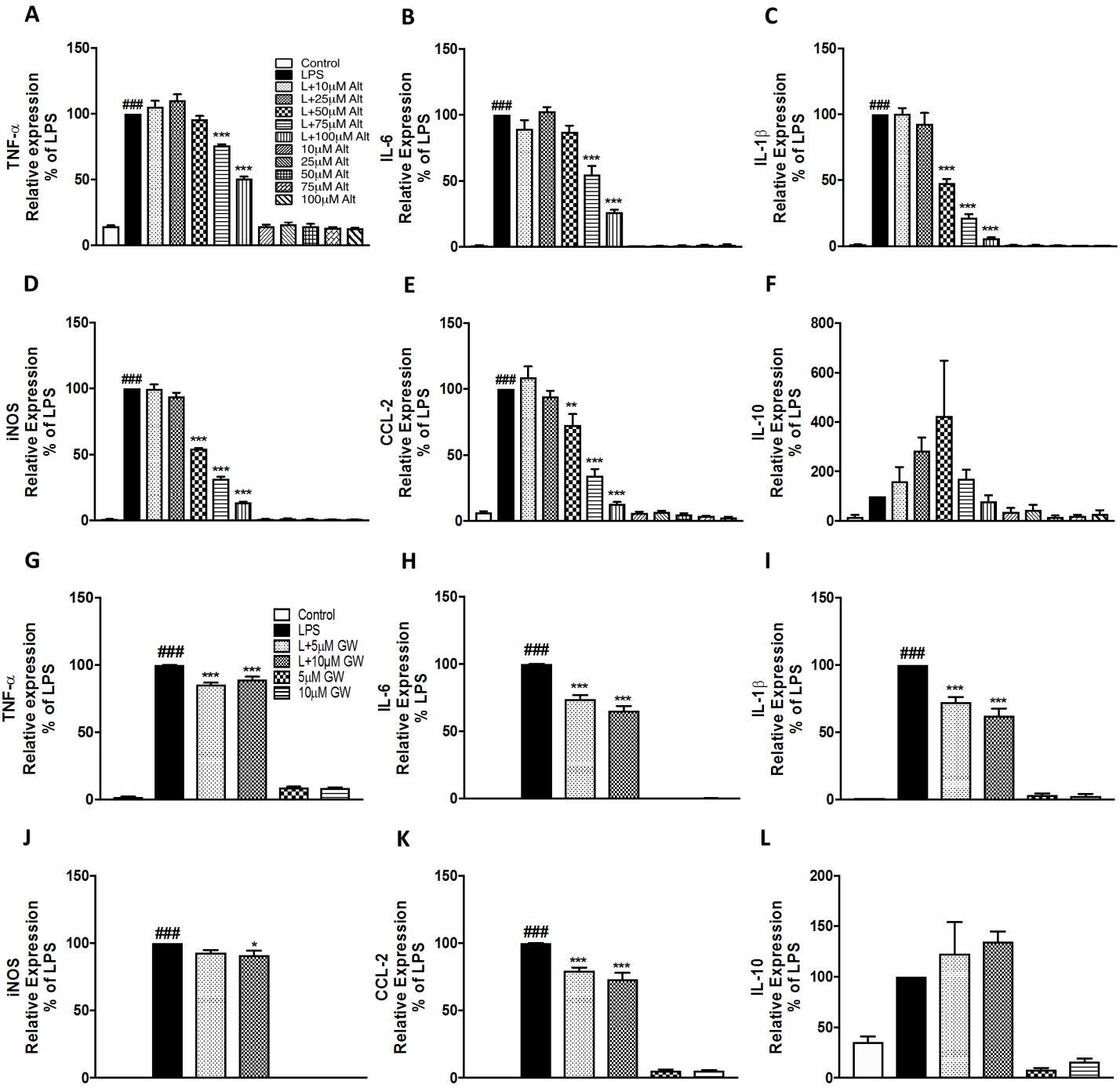

Fig. 2

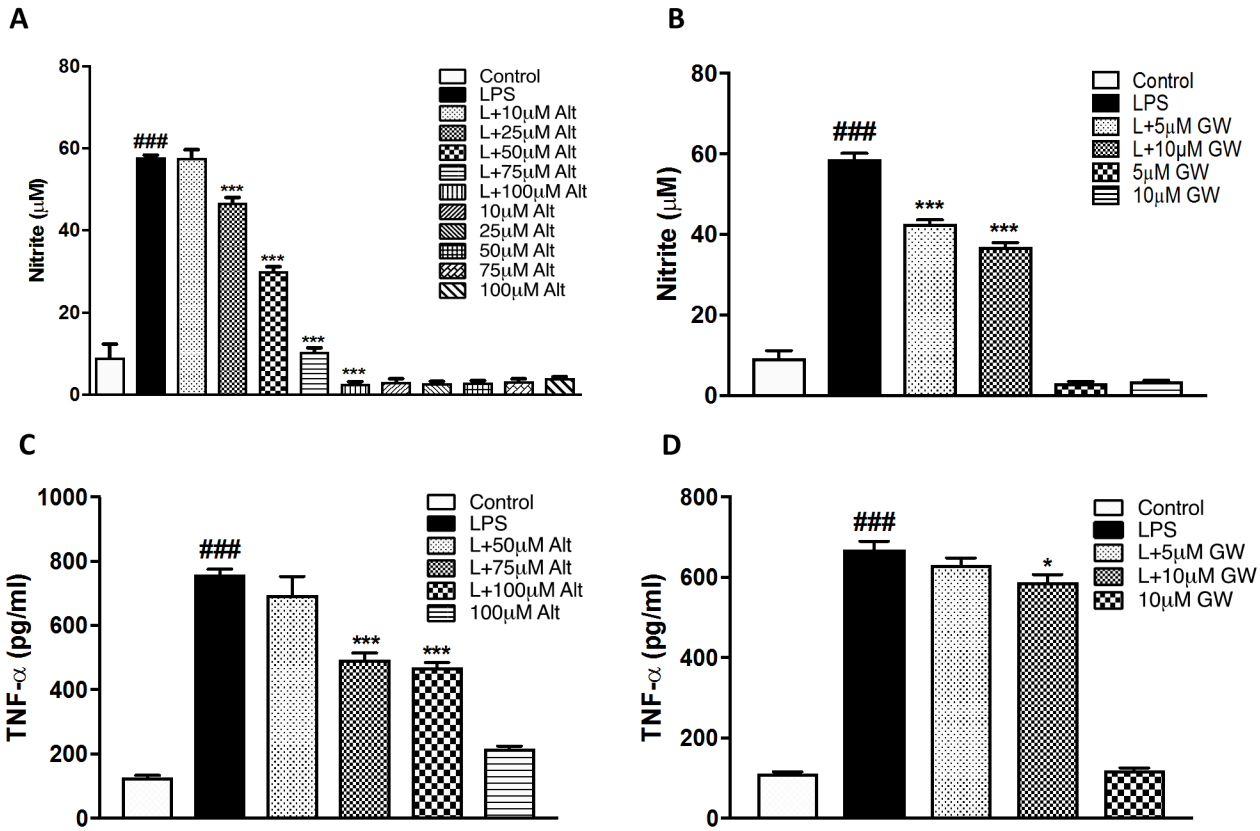

Fig. 3

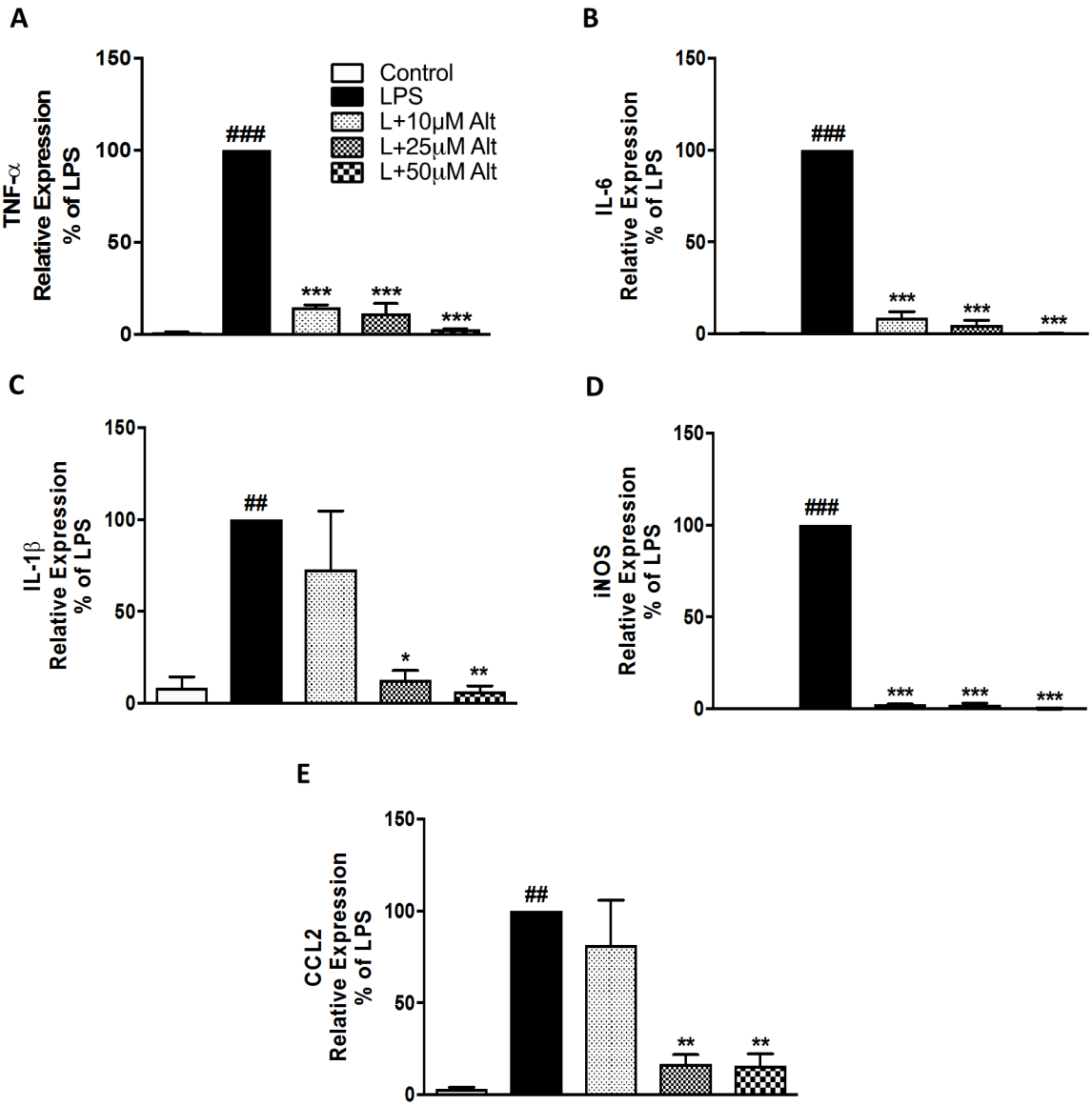

Fig. 4

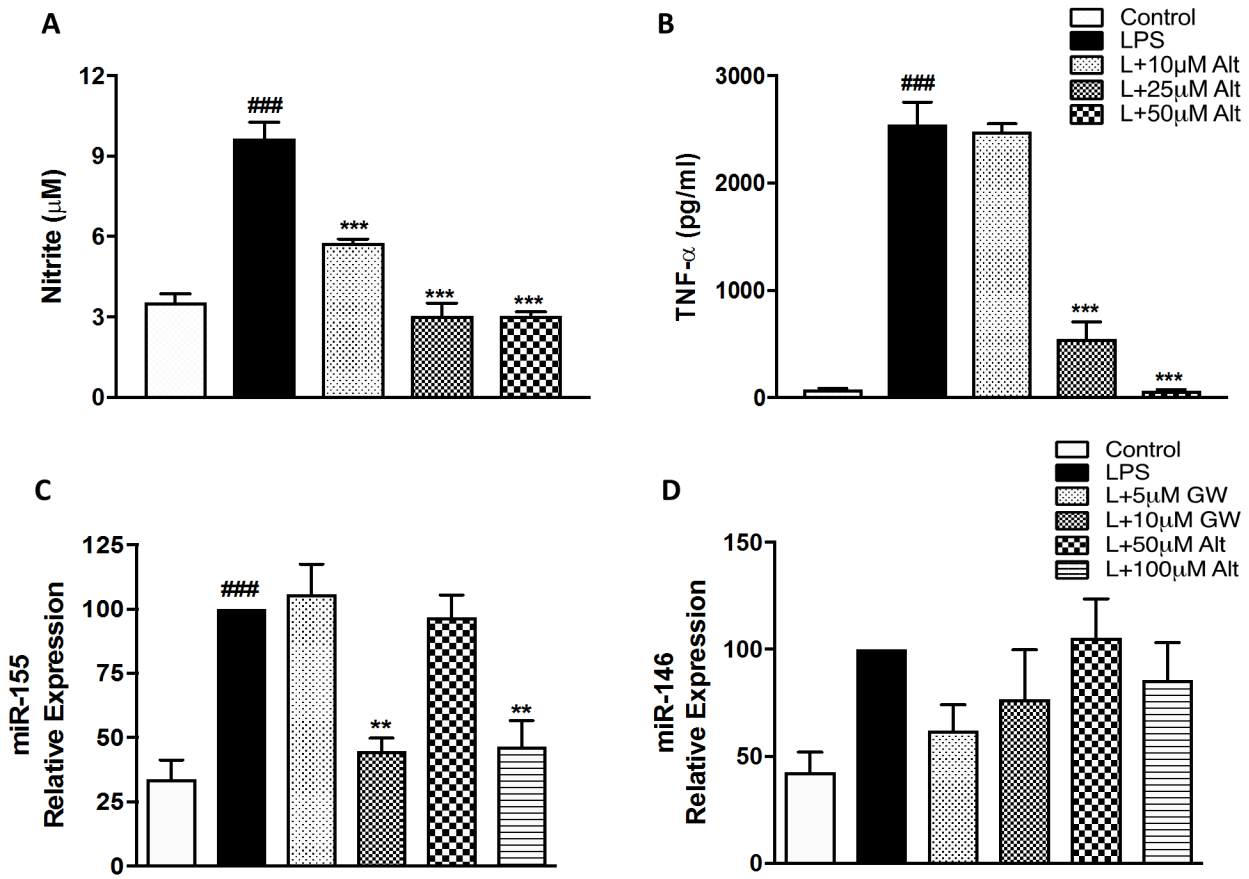

Fig. 5

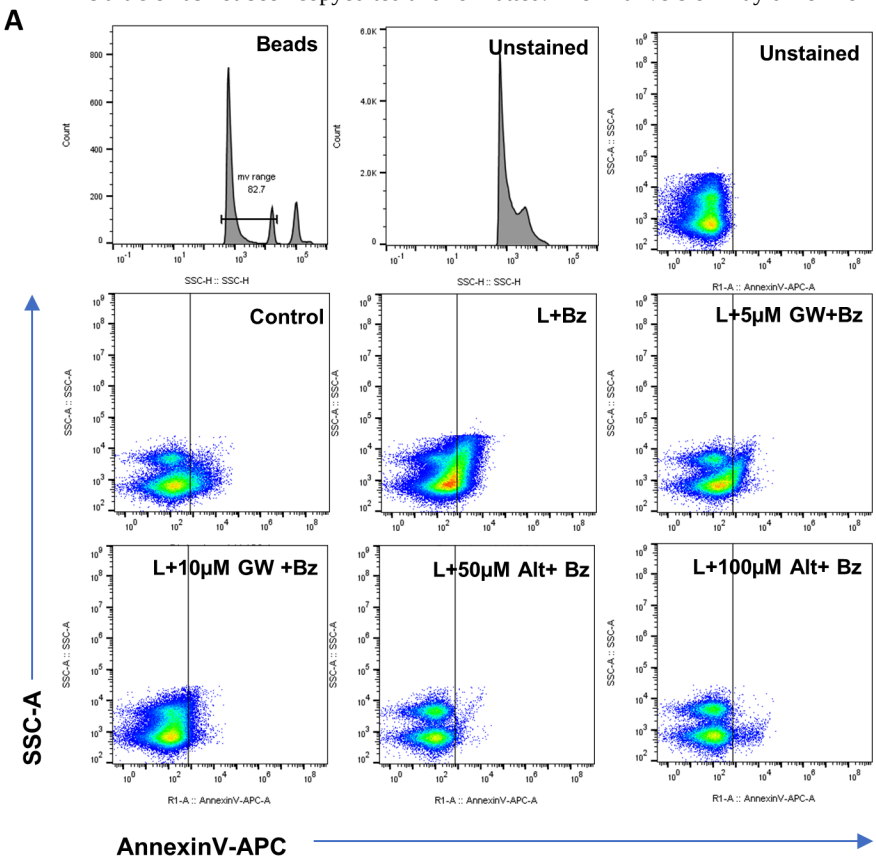

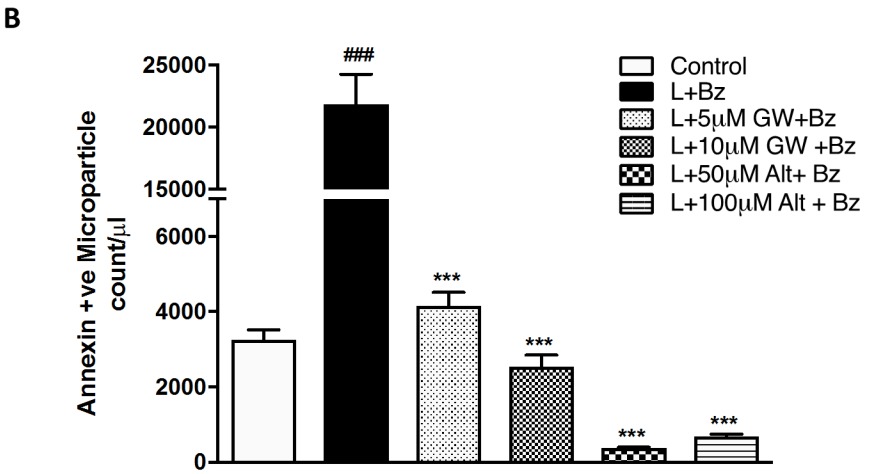

Fig. 6

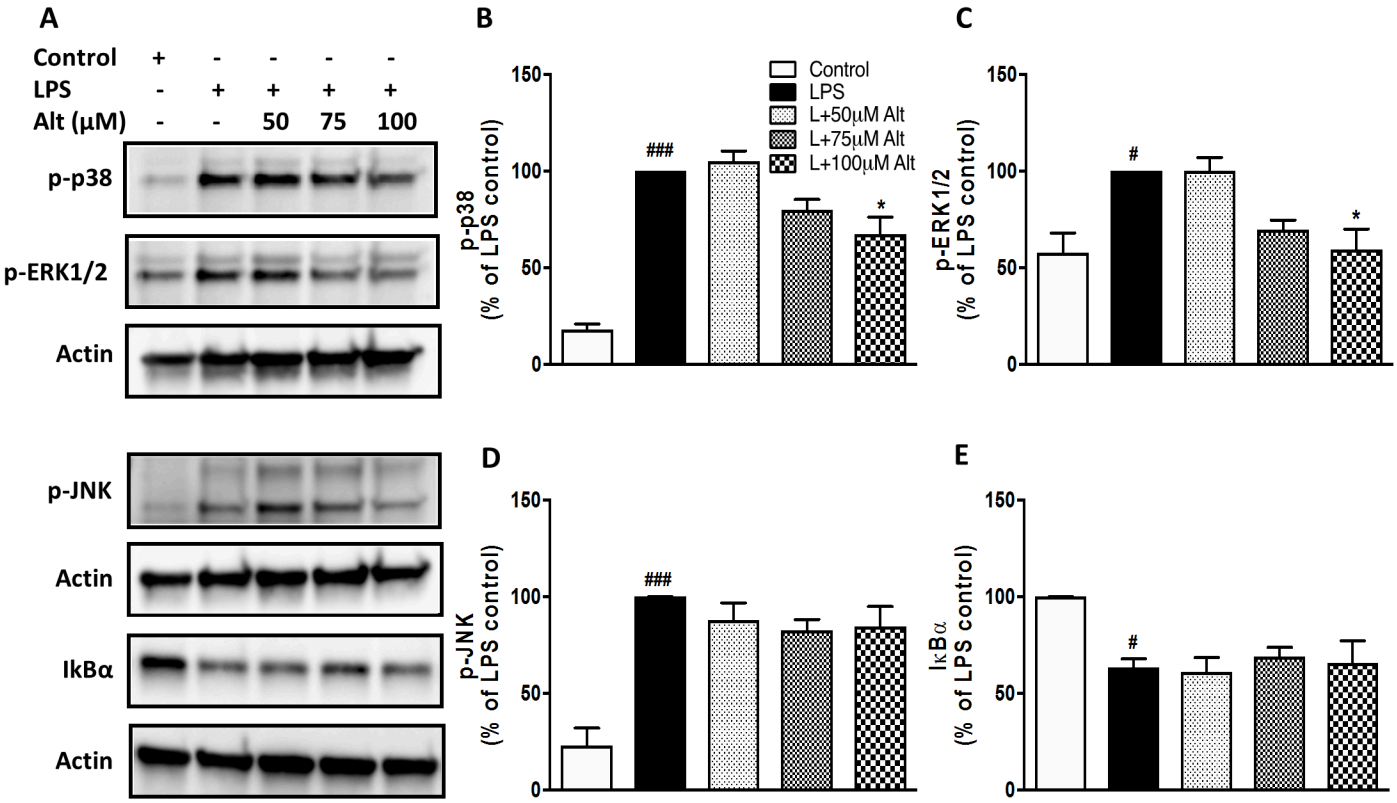

Fig. 7

JPET Fast Forward. Published on December 18, 2018 as DOI: 10.1124/jpet.118.253955

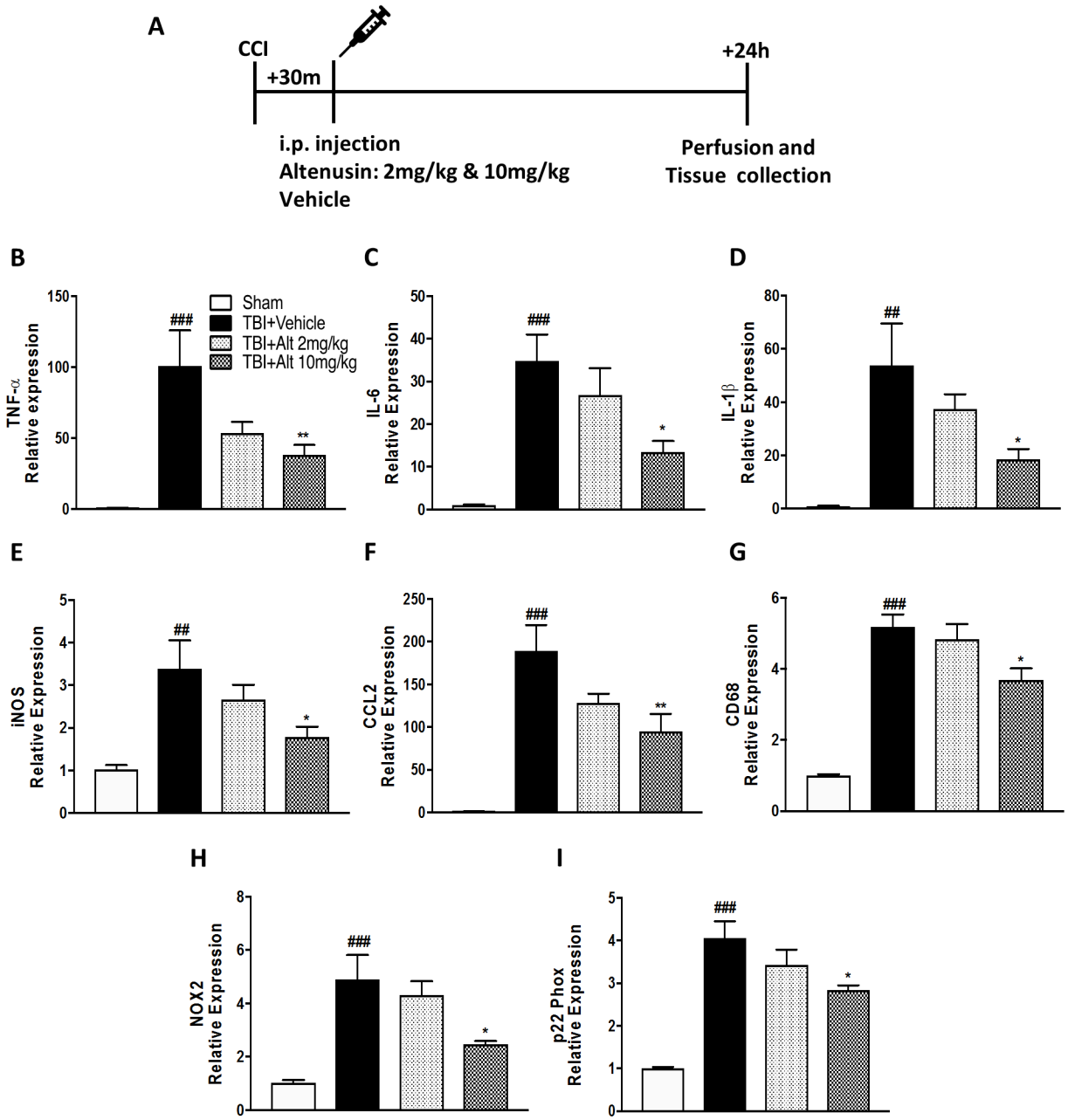

Fig. 8

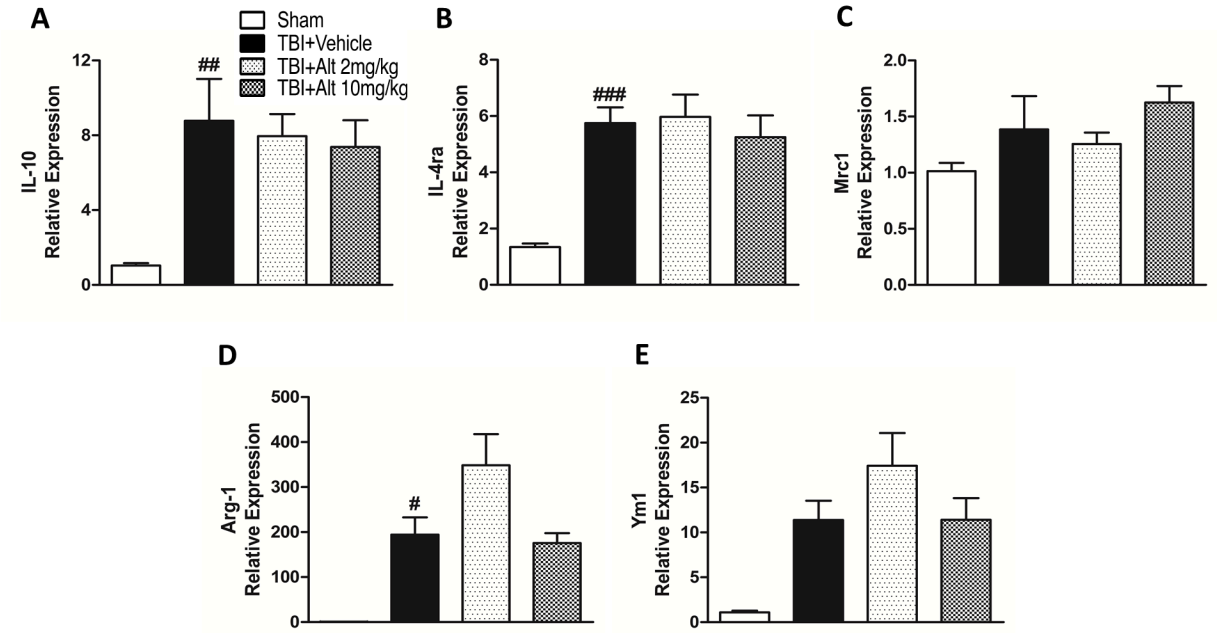

Fig. 9